Photovoltaic Water Pumping Systems Based on Standard Frequency Converters

Alberto Kisner Scortegagna

Dissertation presented to the School of Technology and Management of Polytechnic Institute of Bragança to the Fulfillment of the Requirements for the Master of Science Degree in Renewable Energy and Energy Efficiency, in the scope of Double Degree with Federal University of Technology - Paraná

Supervised by:

Professor Ph.D. Américo Vicente Teixeira Leite

Professor Ph.D. Paulo Cícero Fritzen

This work does not include the appointments and suggestions of the Juri

Bragança

2019

Photovoltaic Water Pumping Systems Based on Standard Frequency Converters

Alberto Kisner Scortegagna

Dissertation presented to the School of Technology and Management of Polytechnic Institute of Bragança to the Fulfillment of the Requirements for the Master of Science Degree in Renewable Energy and Energy Efficiency, in the scope of Double Degree with Federal University of Technology - Paraná.

Supervised by:

Professor Ph.D. Américo Vicente Teixeira Leite

Professor Ph.D. Paulo Cícero Fritzen

This work does not include the appointments and suggestions of the Juri

Bragança

2019

Dedication

To my beloved parents,

Adalberto Scortegagna and Diones Kisner Scortegagna.

Acknowledgment

To God, for always enlightening my path.

To my parents and my sister, who always supported me unconditionally and made this opportunity possible.

To Bruna Teixeira de Freitas, who always supported me.

To the Federal University of Technology - Paraná (UTFPR), Campus Curitiba and the Polytechnic Institute of Bragança (IPB) for the opportunity and for all the effort made by the institutions to make this research opportunity possible.

To Professor Vicente Leite and Paulo Fritzen, who are exceptional professionals and supervisors. I could not expect better supervisors.

To Professor José Baptista, Wellington Maidana, Dionizio Roman, Matheus Montanini Breve and the other friends from the laboratory for the assistance provided.

To my friends that supported and somehow helped me.

Abstract

Photovoltaic water pumping systems are commercialized as closed sets of specific components (kits) at a high cost. Nevertheless, it is possible to develop solutions based on standard components, reliable, widely available and cheaper. These solutions use standard frequency converters and AC pumps. Although it is possible to connect a high voltage photovoltaic string directly to a standard frequency converter, the string becomes oversized for low power applications, bellow several hundreds of Watts.

This work develops and validates new approaches for low power applications using only up to four photovoltaic modules. The first approach uses up to 4 photovoltaic modules, charge controller, battery, battery inverter, frequency converter and a single-phase pump. The second approach uses a developed boost converter to replace the charge controller, battery and battery inverter. For the first approach, several configurations were tested based on different battery voltage levels (12, 24 and 48V) and technologies.

These two approaches were validated successfully. Their results have shown that it is possible to make a system based on standard frequency converters, proving their value for small companies to develop their own cost-effective solutions due to the lower cost, modularity, and availability worldwide. This work was made in cooperation with Valled Soluções Energéticas and CHL Engenharia e Distribuição, which are small companies with experience in photovoltaic lighting and water pumping systems.

Keywords: Photovoltaic Pumping, Frequency Converter, AC pump, Photovoltaic Energy, Boost Converter.

Resumo

Os sistemas de bombagem fotovoltaica são comercializados como kits a um alto custo. No entanto, é possível desenvolver soluções baseadas em componentes convencionais, confiáveis, amplamente disponíveis e mais baratas. Essas soluções usam conversores de frequência e bombas AC. Embora seja possível conectar uma string fotovoltaica de alta tensão diretamente a um conversor de frequência, a string se torna superdimensionada para aplicações de baixa potência, abaixo de algumas centenas de Watts.

Este trabalho desenvolve e valida novas abordagens para aplicações de baixa potência usando no máximo quatro módulos fotovoltaicos. A primeira abordagem utiliza até 4 módulos fotovoltaicos, controlador de carga, bateria, inversor de bateria, conversor de frequência e uma bomba monofásica. A segunda abordagem usa um conversor boost desenvolvido para substituir o controlador de carga, bateria e inversor de bateria. Para a primeira abordagem várias configurações foram testadas com base em diferentes níveis de tensão da bateria (12, 24 e 48V) e tecnologias.

Estas duas abordagens foram validadas com sucesso. Seus resultados mostraram que é possível fazer um sistema baseado em conversores de frequência convencionais, provando seu valor para pequenas empresas desenvolverem suas próprias soluções econômicas devido ao menor custo, modularidade e disponibilidade em todo o mundo. Este trabalho foi realizado em cooperação com a Valled Soluções Energéticas e a CHL Engenharia e Distribuição, pequenas empresas com experiência em iluminação e sistemas de bombagem fotovoltaica.

Palavras-chave: Bombagem fotovoltaica, Inversor de frequência, Bomba AC, Energia Solar Fotovoltaica, Conversor Boost.

Contents

Acknowledgment **vii**

Abstract **ix**

Resumo **xi**

1 Introduction **1**

1.1 Problem Formulation 1

1.2 Objectives 2

1.3 Document Structure 3

2 State of the Art **5**

2.1 Photovoltaic Water Pumping Systems 7

2.1.1 Commercial Photovoltaic Water Pumping Systems 7

2.1.2 Photovoltaic Water Pumping Systems Based on Standard Components 7

3 Proposal of New Approaches for Low Power PVWPS **11**

3.1 PVWPS Based on SFCs with Batteries 11

3.1.1 Challenges on PVWPS Based on SFCs with Batteries 13

3.2 PVWPS based on SFCs without batteries 22

3.2.1 DC-DC Converter 22

3.3 Challenges on PVWPS Based on SFCs (With or Without Batteries) 31

4 Validation with Hardware **39**

4.1 Tests 39

4.1.1 PVWPS Based on SFCs with Batteries 39

4.1.2 PVWPS based on SFCs without batteries 57

5 Conclusions and Future Work **63**

5.1 Conclusions 63

5.2 Future Work 64

A Operation data from tests **A1**

List of Tables

2.1 Invertek Optidrive E3 SFC Rated Operating Voltage Range 9

3.1 V_{bat} and V_{out} relation. 18
3.2 V_{bat} and V_{out} relation with SOC. 18
3.3 Components Used in the Boost Converter 27

4.1 Equipment used in the experimental platform. 40
4.2 Test Summary. 40
4.3 Basic parameters attributed values. 44
4.4 Exclusive parameters in tests A, B, C, D and E. 45
4.5 Exclusive parameters in tests F and G. 45
4.6 Parameters attributed values. 58

List of Figures

2.1 World, Primary energy production(TWh) vs Year [8]. 5
2.2 Access to electricity, rural (% of rural population) [10]. 6
2.3 Access to drinkable water [11]. 6
2.4 Structural outline of PVWPS [5]. 8
2.5 Basic structure of a three(single)-phase SFC. 9

3.1 Basic configuration of a PVWPS, for low power applications, based on the integration of a charge controller, a battery, a battery inverter and a SFC. 12
3.2 Number of cycles vs. extracted capacity (DOD) [17]. 13
3.3 Pump speed control with pump speed as feedback and battery voltage as setpoint. 14
3.4 Control conections in the SFC. 14
3.5 SOC vs f_{out} relation.. 15
3.6 Pump speed control with battery voltage as feedback and battery voltage reference as setpoint. 15
3.7 Control conections in the SFC. 16
3.8 SFC connections description [18]. 17
3.9 Battery voltage measurement using a voltage divider. 18
3.10 Working behavior of the charge controller in the "Power ON/OFF" mode. Adapted from [19]. 19
3.11 Working behavior of the charge controller in the "Power ON + Timer" mode [20]. 20

3.12 Example of the conection with the relay to turn off the battery inverter during the night. 20

3.13 Example of how the irradiance affect the characteristic curve of a solar module [21]. 21

3.14 Example of how the temperature affect the characteristic curve of a solar module [21]. 22

3.15 PVWPS for low power applications with the control conections, using a power boost converter and a SFC. 23

3.16 Topology of the boost converter. 23

3.17 Stage one of the boost converter in continuous mode (switch ON) 24

3.18 Stage two of the boost converter in continuous mode (switch OFF) 24

3.19 Voltage in the inductor of the boost converter in continuous mode vs time. 25

3.20 $\frac{V_o}{V_i}$ x Duty cycle ideal and real in a boost converter. 26

3.21 TL494 PWM Controller [23]. 28

3.22 Boost converter and the schematic of the control circuit. 29

3.23 Control scheme of the SFC using the macro PID, and the DC-Link voltage as process variable, to control the speed of the pump. 31

3.24 Macro functions of PI control mode [18]. 33

3.25 Exemple of a buoy valve instaled [24]. 36

3.26 Overload protection in the Invertek Optidrive E3. Adapted from [18]. . . . 36

3.27 Exemple of a electrical buoy. 37

4.1 Pumps used in the tests, (A) Pentax CR100/00/1 1HP, (B) Sterwins 750 DW-3 1HP. 41

4.2 PV Modules used in the tests, (A) REC 275PE 275W, (B) Fluitecnik FTS-220P 220W. 42

4.3 Battery inverters used in the tests, (A) Cotek 12VDC-230VAC-600W Pure Sine, (B) HQ 24VDC-230VAC-600W Modified Sine, (C) Carspa 12VDC-230VAC-1000W Modified Sine, (D) Epever SHI 3000 48V-230V-3000W Pure Sine, (E) Epever SHI 3000 48V-230V-3000W Pure Sine. 42
4.4 Charge controllers used in the tests, (A) Epever IT4415ND MPPT, (B) Steca PR2020 PWM. 43
4.5 SFC used in the tests: Invertek Optidrive E3 1HP Single-Phase Input/Output. 43
4.6 Batteries used in the tests, (A) MasterBat MBG100Ah-12V, (B) Ultracell UCG 20-12, (C) Sonnenschein S12/17 G5. 44
4.7 Platform of test C. 47
4.8 Platform of test E. 50
4.9 Experimental platform for low power applications based on the integration of a charge controller, a battery, a battery inverter and a SFC. 52
4.10 One day of operation of a low power applications based on the integration of a charge controller, a battery, a battery inverter and a SFC. A) Irradiation in Bragança vs hours (02/05/2019); B) Speed of the pump vs hours (02/05/2019). 53
4.11 One day of operation of a low power applications based on the integration of a charge controller, a battery, a battery inverter and a SFC. A) Irradiation in Bragança vs hours (02/04/2019); B) Speed of the pump vs hours (02/04/2019). 54
4.12 Shadow produced by a small wind turbine (02/04/2019 - 10:45). 55
4.13 Experimental platform for low power applications based on the integration of a charge controller, a battery, a battery inverter and a SFC. 56
4.14 Two hours operation of a low power applications based on the integration of a charge controller, a battery, a battery inverter and a SFC. A) Irradiation in Bragança x hours (13/05/2019); B) Speed of the pump x hours (13/05/2019). 57
4.15 Experimental platform for low power applications based on the integration of a boost converter and a SFC. 59
4.16 Voltage, seen throught a voltage divider, in the input of the SFC stable in 350 VDC before the pump starts 60

4.17 Voltage, seen throught a voltage divider, in the input of the SFC stable bellow 350 VDC with the pump working and the pulses in the IGBT . . . 60
4.18 Voltage, seen throught a voltage divider, in the input of the SFC stable in 350 VDC after the pump stops 61
4.19 One hour of operation (irradiation and pump speed in Bragança at 15/05/2019) of a low power applications based on the integration of a boost converter and a SFC 61

Acronyms

DOD Deep of discharge.

$\mathbf{K}_p$ Proportional gain.

MPP Maximum power point.

MPPT Maximum power point tracking.

PI Proportional integral.

PID Proportional integral derivative.

PLC Programmable logic controller.

PV Photovoltaic.

PVWPS Photovoltaic water pumping system.

PWM Pulse width modulation.

SFC Standard frequency converter.

SOC State of charge.

STC Standard test conditions.

$\mathbf{T}_i$ Integrative time.

$\mathbf{V}_{bat}$ Battery voltage.

$\mathbf{V}_{oc}$ Open-circuit voltage.

$\mathbf{V}_{out}$ Output voltage.

VMPP Maximum power point voltage.

WHO World Health Organization.

Chapter 1

Introduction

In 2015 the World Health Organization (WHO) affirmed that only 71% of the world population had access to drinkable water, and it is estimated that in 2025 half of the population will be living in areas with hydric stress. From the WHO data it is clear that most of these areas of poor water service are located between the tropics [1].

In this global context, there is the initial challenge of this work: The lack of drinkable water to a big part of the world population, being the most of this population with this problem situated between the tropics. One solution is to pump water from the underground, but electricity may not be available in these places. Due to the fact that the electricity is not accessible in many places, conventional solutions such as manual pumps, water pump coupled with combustion engines or windmills are used. Despite that, it is possible to use Photovoltaic water pumping system (PVWPS) [2]. This work presents new, cheaper and feasible approaches to PVWPS.

1.1 Problem Formulation

Some multinational companies, seeing the demand for pumping systems and the lack of electricity, already developed closed kits to integrate Photovoltaic (PV) energy and pumping. However, usually, these kits have high costs and use specific parts, like DC pumps and dedicated controllers. Since small or very small companies do not have the

capability to develop a dedicated product, they are dependent on the systems developed by multinationals. Although they can develop innovative and cost-effective solutions using off-the-shelf components, such as Standard frequency converter (SFC) and AC water pumps [2].

SFCs are designed to work connected to grid, but previous works demonstrated that if a PV string provides a DC voltage of the order of 350 V to a single-phase input SFC it will work [3] [4]. Despite the possibility to connect the PV string directly to the SFC, this would make the applications with pumps of just some hundreds of watts oversized in terms of the power of modules and structure. In fact many applications only need a pump of some hundreds watts and some hours of operation is related to the existence of a natural relation between the need of water pumping and the availability of solar irradiance [5] [6] [7] [2].

This work presents solutions for PVWPS based on SFC for different power levels, and proposes two new approaches for low power applications, using only three or four PV modules, a single-phase input/output SFC and a conventional AC Pump. Some of these solutions are valuable for small and very small companies to develop their own and cost-effective solutions. This work comes from the cooperation and challenge of VALLED Soluções Energéticas and CHL Engenharia e Distribuição companies [2].

1.2 Objectives

The focus of this project is to research of PVWPS available on the market and to develop alternative and competitive low power systems (less than 1 kW), based on standard frequency converters and standard components in general. The objectives can be summarized as follows:

- Connect a PV string to a SFC, for low power applications.
- Reduce the number of PV modules necessary to supply the load.
- Test several standard components.

- Implement a solution to solve the lack of Maximum power point tracking (MPPT) in SFC.
- Control the pump speed according to the irradiance level.
- Implement a solution to solve the cases of instability due to a sudden fall of irradiance, lack of protections against empty well and full tank states.
- Avoid batteries as energy storage components.
- Provide solutions with low cost and reliability.

This work presents solutions for PVWPS based on SFC for low power levels, and proposes a new approach for low power applications, using up to four PV modules.

1.3 Document Structure

This dissertation is divided into five chapters, to describe the work developed through the research.

Chapter 1 contains an introduction to PVWPS, the context that it is inserted and the problem formulation.

Chapter 2 presents the current context in the world, the state of the art of PVWPS including the traditional commercial solutions and the PVWPS based on standard components.

Chapter 3 contains two new approaches proposed for low power PVWPS, with the description of how the system works.

Chapter 4 presents the validation of the two new approaches proposed for low power PVWPS.

The conclusions and suggestions for future works are in Chapter 5.

Chapter 2

State of the Art

The energy consumption of the world is rising every year [8], as shown in Fig. 2.1. However, most of the energy is provided by non-renewable sources and these sources generally are not cheap. With the high dependence on non-renewable sources, the tendency is the price rise by supply and demand. In this context, renewable energies can take advantage, as the photovoltaic (PV) energy for instance. The solar radiation is abundant, free, enduring and unpolluted [9], making it a great alternative to substitute at least a good part of the energy dependence in the world.

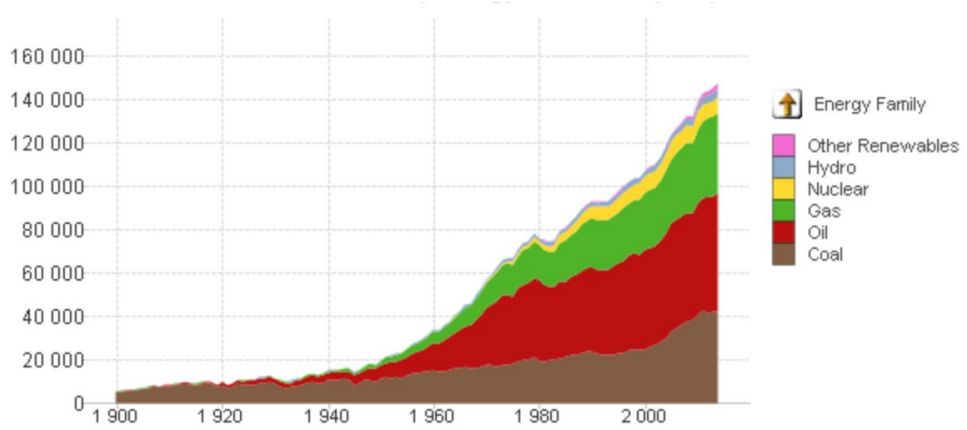

Figure 2.1: World, Primary energy production(TWh) vs Year [8].

Although the energy is almost a necessity to all humankind, it is not necessarily available in all areas. Fig. 2.2 shows that in rural areas this lack of electrical energy affects

several places, even in current days [10].

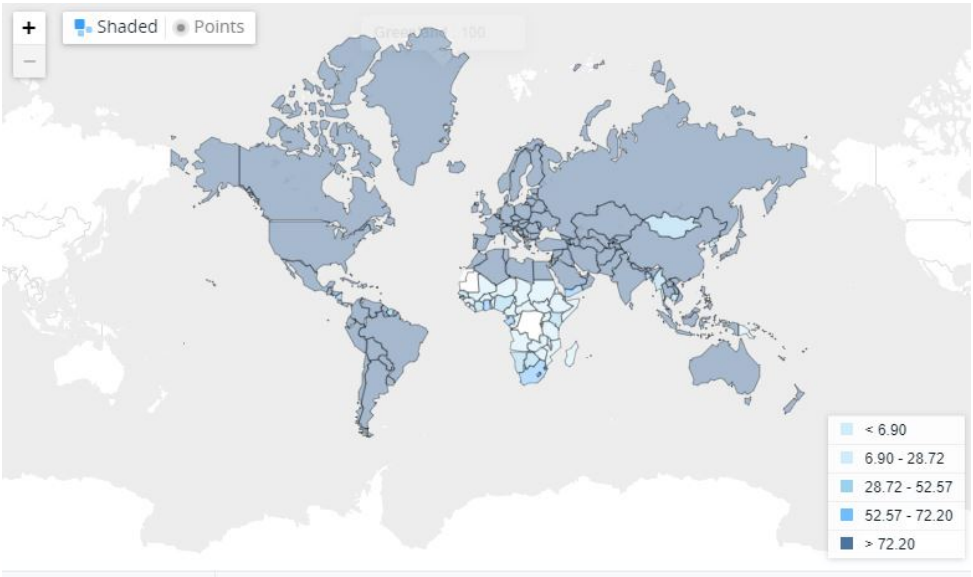

Figure 2.2: Access to electricity, rural (% of rural population) [10].

A necessity that is not available to all people too is access drinkable water [1]. Fig. 2.3 shows that this lack of water affects several places [11]. To have water in these places most of the time the only option is pump water from the underground. Traditionally the solution to pump water is through hand pump or buckets in wells [12].

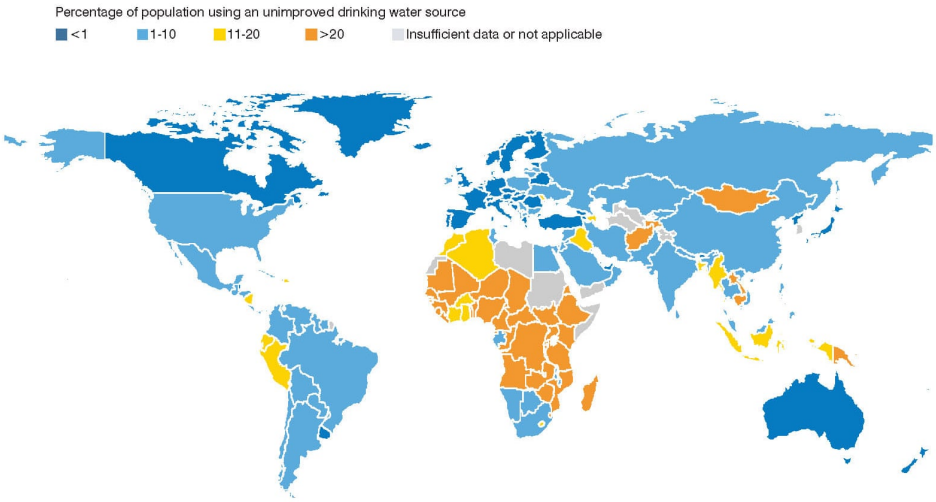

Figure 2.3: Access to drinkable water [11].

Comparing Fig. 2.2 and 2.3 it is possible to see that a good part of the areas with

problems with drinkable water are the same that have problems with energy. Most of these areas are between the tropics, which make these areas perfectly suitable to Photovoltaic Water Pumping Systems (PVWPS). As a matter of fact, there is a natural correlation between the necessity of pumping systems and the high availability of solar radiation [7].

2.1 Photovoltaic Water Pumping Systems

2.1.1 Commercial Photovoltaic Water Pumping Systems

Probably noticing the correlation between the high availability of solar radiation and the necessity of pumping systems big companies developed and distributed their own solutions. Although these solutions are efficient and most of them have maximum power point tracking (MPPT) [13], they have high cost and use specific components, such as dedicated controllers and DC pumps. The fact that these commercial kits use specific components make small companies dependent on that specific company, due to the fact that they can not develop a dedicated solution. Despite that, it is possible to develop new solutions based on standard components such as Standard Frequency converter (SFC) and AC pumps, widely available on the market and cheaper than the kits.

The basic block diagram of a PVWPS is described in Fig. 2.4. The structure is basically the PV modules connected to a controller that supplies energy to the electric pump.

2.1.2 Photovoltaic Water Pumping Systems Based on Standard Components

The use of a standard component, as a SFC in a PVWPS, is advantageous compared to dedicated equipment. This advantage is due to standard components being widely available in the market for all power ranges, as well as being reliable, cost-effective, durable and have ample production by a lot of manufacturers. Another large advantage of using SFC is that for a pump power in the order of some kW or higher it is possible to connect the SFC directly to the PV string [3]. However, the problems of applying SFC in PVWPS

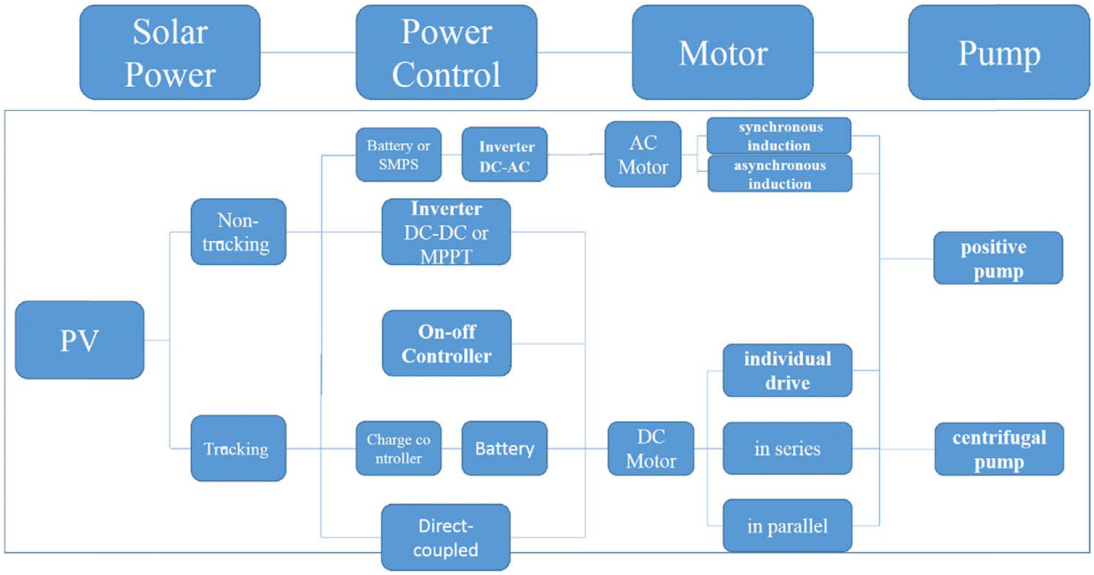

Figure 2.4: Structural outline of PVWPS [5].

are well-known, for instance: abrupt fall of irradiance, unavailability of maximum power point tracking (MPPT) and lack of protection in cases when the pump is operating without water or pumping to a full tank [6] [2].

Although this solution based on SFC has not MPPT to adjust the setpoint automatically, the literature present some solutions: An analog MPPT tracker [14]; Programmable logic controller (PLC) to track the Maximum power point (MPP) and protect from empty and full tank states [4]; an analog circuit based on the low-cost temperature sensor LM35 [3]; a MPPT charger controller with batteries and a battery inverter [15] [2].

The topology of a SFC can be separated into two power stages: A rectifier bridge for AC/DC conversion and a DC/AC converter. Between these two stages, there is a DC-link with a high voltage DC capacitor bank. An illustration of the blocks of an SFC is shown in Fig. 2.5. Normally, the SFC is powered by the grid with constant voltage and frequency. Nevertheless, if the PV string can supply the DC voltage, described in the Table 2.1, it is possible to set the single-phase input SFC to control the pump according to the input voltage, which reflects the irradiance [3] [16] [2].

Considering a conventional PV module of 330 W with a typical Open-circuit voltage

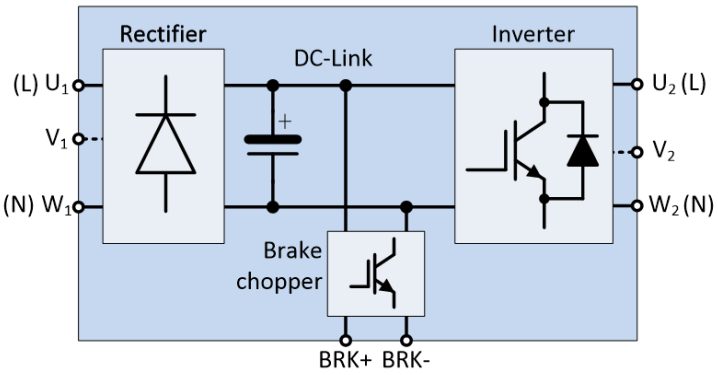

Figure 2.5: Basic structure of a three(single)-phase SFC.

Table 2.1: Invertek Optidrive E3 SFC Rated Operating Voltage Range

AC Input Voltage (L-N)	$\sim 200 - 240V \pm 10\%$
DC-link Voltage (Single-phase Input)	$\sim 283 - 342V \pm 10\%$
DC-link Voltage (Three-phase Input)	$\sim 566 - 679V \pm 10\%$

(V_{oc}) of 46 V, a PV string with a maximum of 7 PV modules is recommend for a single-phase SFC due to the V_{oc} of 322 V. The total power will be 2,31 kW, making it suitable for applications with the power magnitude of 1.5-2 kW. The set point, i.e., the DC link operating voltage should be close to the Maximum power point voltage (VMPP) of the PV string, under Standard test conditions (STC) [3]. In this case, 266 V. Considering the period of operation and the effect of the temperature, the previous setpoint should be the voltage at the maximum temperature [4], [2].

The DC-link voltage is the process variable controlled in a closed loop by the Proportional integral (PI) Controller macro or Proportional integral derivative (PID) Controller of the SFC. In the case of the Invertek Optidrive E3, it is the PI Controller macro. Thus it is necessary to set the Proportional gain (K_p) and the Integrative time (T_i), which will determine the dynamic of the system. The measure of the DC-link voltage is given by the SFC and the reference value has to be set in a potentiometer or by a parameter. It is also required to set other operating parameters, as inputs, outputs, acceleration and deceleration times [4], [2].

As previously stated, these discussed solutions are good for powers higher than 1.5

kW. However, in many applications the needed power is smaller, making this number of modules oversized for the application only with the objective of achieving high voltage. For example: For a pump of 1 HP (about 750W), three or four modules could be enough if the voltage were higher. The next section presents two approaches for low power applications, using a SFC and up to three or four modules [2].

Chapter 3

Proposal of New Approaches for Low Power PVWPS

For photovoltaic water pumping systems (PVWPS), where the power generated by three or four PV modules is enough, innovative solutions can be developed, still based on standard frequency converters (SFCs) and conventional AC Pumps. As mentioned in the section, a SFC has to be powered with a minimum voltage of 200 VAC or 283 VDC, therefore, the input voltage must be boosted. Considering this, two major practical approaches are proposed next [2].

To these approaches were considered the use a single-phase input/output SFC of Invertek: Optidrive E3 of 1 hp. This option was made due to the fact that for 1kW or less single-phase pumps are more common.

3.1 PVWPS Based on SFCs with Batteries

A first practical approach for low power PVWPS based on SFCs is presented in Fig. 3.1. This approach is based on the integration of widely available and cost-effective equipment: charge controller, battery, battery inverter and a SFC [2].

The battery inverter needs to boost the voltage and can be a pure sine wave inverter or a cheaper modified sine wave inverter. It can even be a push-pull DC-AC power module

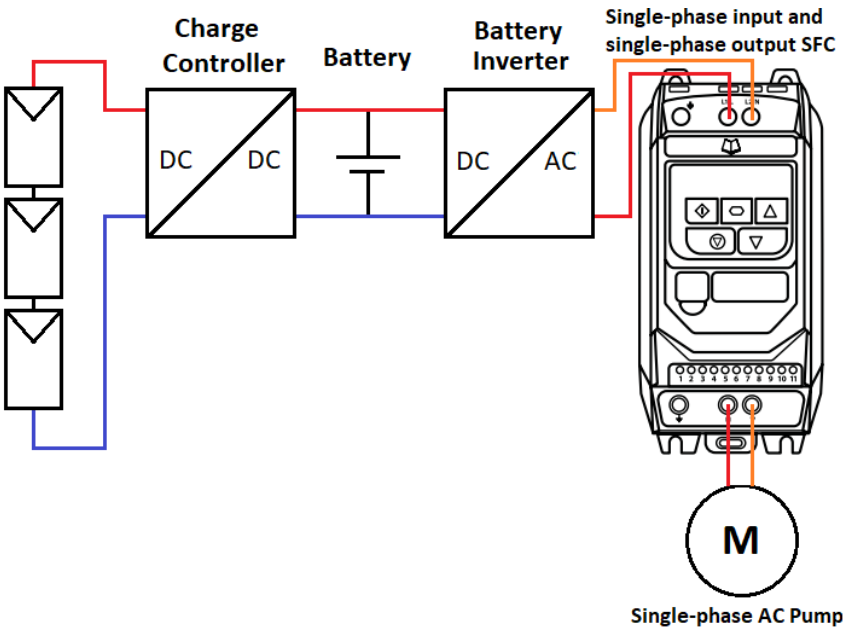

Figure 3.1: Basic configuration of a PVWPS, for low power applications, based on the integration of a charge controller, a battery, a battery inverter and a SFC.

[15]. Since the SFC has a rectifier bridge at the input side, it does not matter if the wave is a pure sine or not. Although, with the push-pull DC-AC power module inverter it is needed an extra rectifier bridge based on fast-recovery diodes considering the high-frequency (such as 20 kHz) output pulses. Schottky diodes can be used for this purpose. Indeed, SFCs are equipped at the input with a rectifying bridge that is not suitable for such high frequencies. Alternatively, a voltage filter can be applied at the output of the DC-AC push-pull inverter [2].

The charge controller can be of the type MPPT or just PWM. Charge controllers with MPPT are more efficient but they are also more expensive. The choice of one or another will depend on the overall size of the system and its requirements. Indeed, in PVWPS, the MPPT may not be a critical issue [2].

To choose the size of the battery there are mainly two perspectives: a high capacity if it is not possible to store water in a tank; or a low capacity if it is possible. The approach of this work is with batteries with a low capacity due to the high cost. Besides, the use of the PID macro available on SFC strongly increases the battery lifetime by limiting the

battery Deep of discharge (DOD) too, e.g., 20%. This way, the battery is used only to permit the use of the charge controller, and not to supply energy [2].

The concept of DOD is how much of the capacity in the battery is extracted, on the other hand, the State of charge (SOC) is how much of the capacity is available. For example, if a DOD is 20% the SOC is 80%.

In this work, the DOD is limited to 20% due to the fact that all batteries, independent on the technology, have the number of cycles increased if the DOD is lower. It is possible to observe in Fig. 3.2 that if this battery works with a DOD of 20% the maximum number of cycles will be approximately 3800, but if the DOD is 50% the maximum number of cycles will be 1200, representing a loss of useful life in the order of 68%. This control of the DOD is possible using the PID macro with a closed loop control of the pump's speed, which is explained in the section 3.1.1.

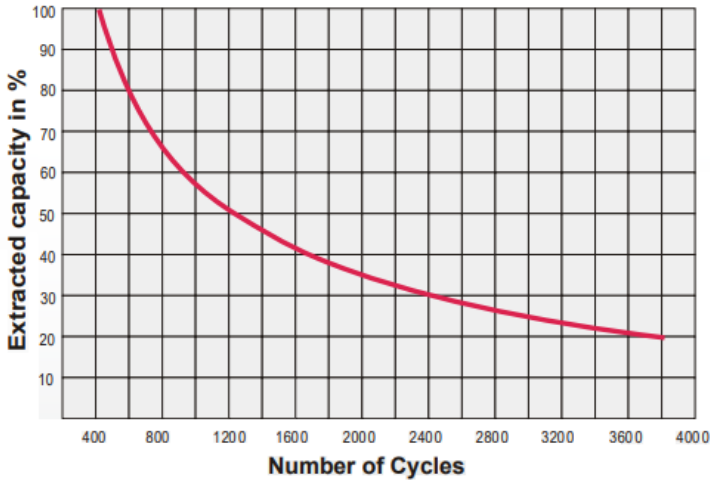

Figure 3.2: Number of cycles vs. extracted capacity (DOD) [17].

3.1.1 Challenges on PVWPS Based on SFCs with Batteries

Possible Closed Loop Controls

The first eligible closed loop control to this application is using the speed of the pump, scaled from 0 V to 10 V, given by the SFC in one of the analog outputs as the feedback,

and the battery voltage, seen through a voltage divider, as the setpoint. This closed loop control is shown in Fig 3.3 and the connections with the SFC in Fig. 3.4 .

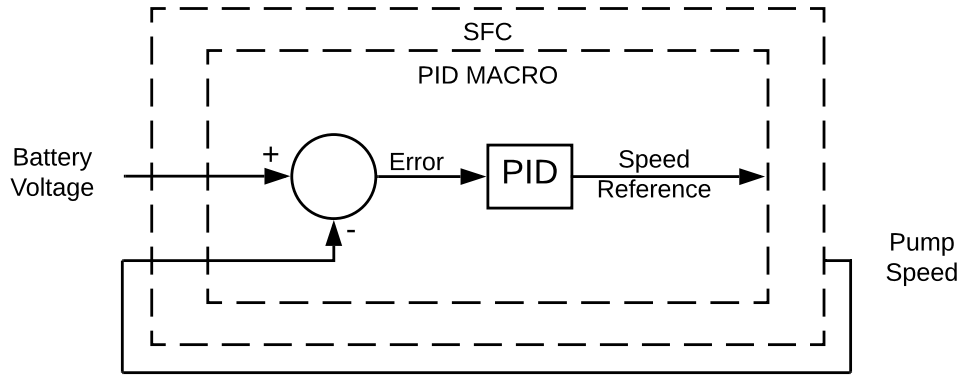

Figure 3.3: Pump speed control with pump speed as feedback and battery voltage as setpoint.

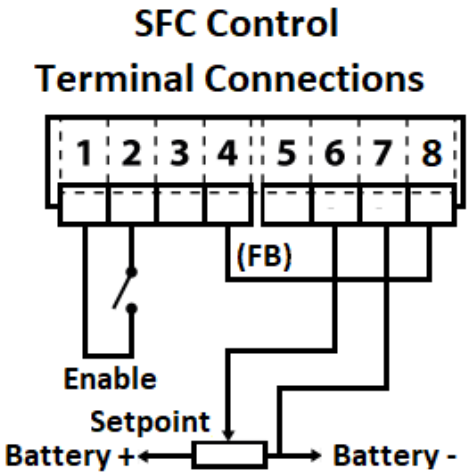

Figure 3.4: Control conections in the SFC.

This control makes the pump work proportionally to the irradiance, working as shown in Fig. 3.5. To let the f_{out} equivalent to the SOC wanted it is necessary to scale the SOC voltage by the parameters P-35 (Analog Input 1 Scaling) and P-39 (Analog Input 1 Offset) in the Invertek Optidrive E3. These parameters set what will be read as 0 and 100%, independently that the voltage divider will present 7 V as the maximum voltage and 5 V as the minimum voltage, for example.

The second eligible closed loop control to this application is to use the battery voltage

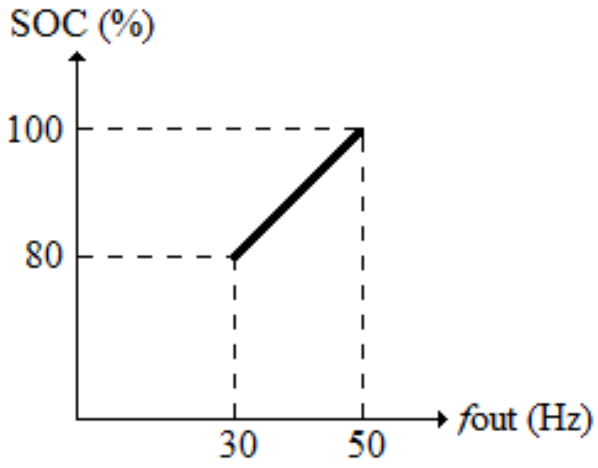

Figure 3.5: SOC vs f_{out} relation..

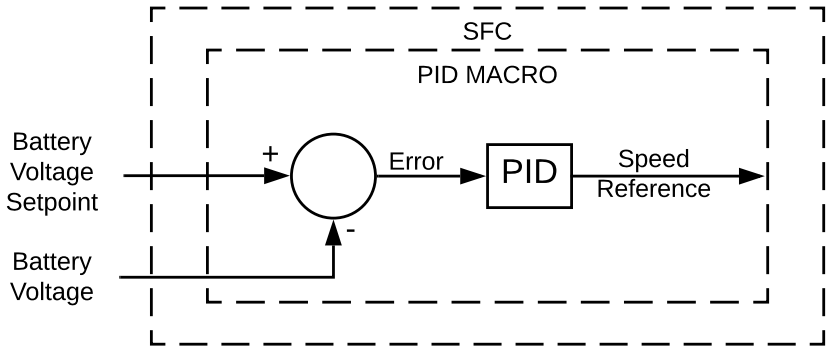

Figure 3.6: Pump speed control with battery voltage as feedback and battery voltage reference as setpoint.

as feedback, and the battery voltage reference as the setpoint. This closed loop control is shown in Fig 3.6 and the connections with the SFC in Fig. 3.7 [2].

This control will basically make the pump work proportional to the irradiance by keeping the voltage in the batteries constant by increasing or decreasing the pump speed, so the battery voltage will always try to stay with the voltage given by the setpoint. The used setpoint is equivalent to 80% of the SOC [2].

In these two closed loop controls it is necessary to use additional parametrization to make the pump completely stop when there is not enough irradiance (a temporary cloud for example) and restart when the irradiance is high enough. The parameters needed are the P-48 (Standby Mode Timer) and P-49 (PI Control Wake Up Error Level). With this

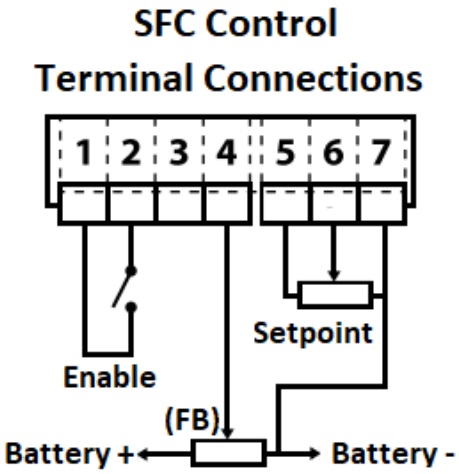

Figure 3.7: Control conections in the SFC.

extra parametrization the Optidrive E3 will enter the standby mode after working the amount of time set in P-48 in the minimum frequency of the pump (P-02). When the SFC enters in standby mode it means that even in the lowest power of the pump the irradiance is not enough to keep the battery voltage above the SOC of 80%. The SFC will only resume normal operation when the error level of the PID is above the error set in P-49.

Battery Voltage Measurement

The two proposed closed loop controls use the battery voltage connected to the SFC. Although it is not possible to make this connection directly due to the limit of the voltage in the analog inputs in the SFC (10V), which can be seen in Fig. 3.8.

In the first proposed closed loop control the analog input 1 is used and in the second is the analog input 2. Both analog inputs have the maximum operating values as 10V and 20mA. Consequently, it is not possible to connect the regular battery voltage used in solar charge controllers, which is 12, 24, 36 and 48 V, directly to the SFC. Noticing this compatibility problem the chosen solution to solve this issue is to use a voltage divider, as shown in Fig. 3.9.

To calculate the Output voltage (V_{out}) the Equation 3.1 was used, which is the equation that expresses the behavior of the voltage divider.

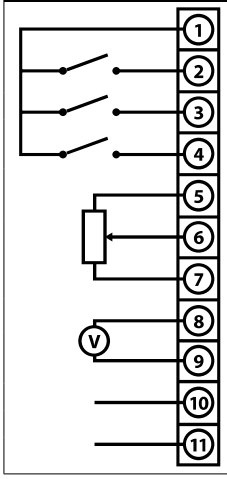

Default Connections	Control Terminal	Signal	Description
	1	+24Vdc User Output	+24Vdc user output, 100mA. Do not connect an external voltage source to this terminal.
	2	Digital Input 1	Positive logic "Logic 1" input voltage range: 8V ... 30V DC "Logic 0" input voltage range: 0V ... 4V DC
	3	Digital Input 2	
	4	Digital Input 3 /Analog Input 2	Digital: 8 to 30V Analog: 0 to 10V, 0 to 20mA or 4 to 20mA
	5	+10V User Output	+10V, 10mA, 1kΩ minimum
	6	Analog Input 1 / Digital Input 4	Analog: 0 to 10V, 0 to 20mA or 4 to 20mA Digital: 8 to 30V
	7	0V	0 Volt Common, internally connected to terminal 9
	8	Analog Output / Digital Output	Analog: 0 to 10V, 20mA maximum Digital: 0 to 24V
	9	0V	0 Volt Common, internally connected to terminal 7
	10	Relay Common	
	11	Relay NO Contact	Contact 250Vac, 6A / 30Vdc, 5A

Figure 3.8: SFC connections description [18].

$$V_{out} = \frac{V_{bat} R_2}{R_1 + R_2} \tag{3.1}$$

Since the experimental part of this work uses voltages of batteries up to 48 V and the voltage applied by the battery charger can go up to 60 V, this was the highest value considered. Using a voltage divider designed for the worse case implies that to use lower battery voltages is just a matter of parametrization in the SFC. By adopting this strategy some mistakes in changing the voltage divider when the battery is changed are avoided, preserving the integrity of the SFC. After all, V_{out} will always stay below 10 V, which is the limit of the SFC.

To simplify the voltage reading in the output of the voltage divider it is considered a proportion 1 to 10. To limit the current through the voltage divider, high values as R_2 = 10 kΩ and R_1 = 100 kΩ were chosen. One point observed was that the value of the internal resistance of the analog input of the SFC is ideally infinite, although in reality that is not true. It is possible that the value of R_2, which is in parallel with the internal resistance of the analog input, can change the relation of the voltage divider. However, this internal resistance did not change the voltage divider. The equation to obtain the output voltage is described in Equation 3.2 and the relation beteewn Battery voltage

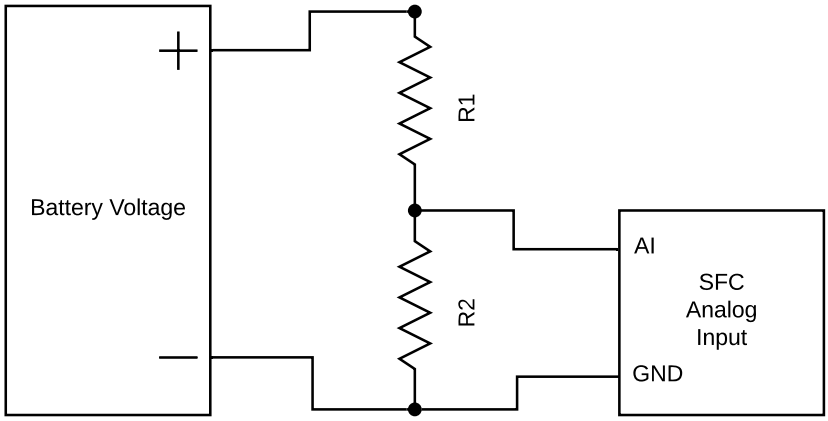

Figure 3.9: Battery voltage measurement using a voltage divider.

(V_{bat}) and V_{out} is shown in Table 3.1. The relation of the main voltages with the SOC are presented in Table 3.2.

$$V_{out} = \frac{V_{bat}10k}{100k + 10k} \tag{3.2}$$

Table 3.1: V_{bat} and V_{out} relation.

V_{bat} (V)	V_{out} (V)
60	6
48	4.8
36	3.6
24	2.4
12	1.2

Table 3.2: V_{bat} and V_{out} relation with SOC.

Main V_{bat} (V)	48	36	24	12
SOC	V_{out} (V_{bat}) (V)			
100%	5.6 (56)	4.2 (42)	2.8 (28)	1.4 (14)
80%	4.88 (48.8)	3.66 (36.6)	2.44 (24.4)	1.22 (12.2)

How to Turn the Frequency Inverter Off at Night

The battery inverter is activated by the charge controller only during sun hours in order to avoid self-consumption of the SFC and inverter during the night. This is possible due to the load output available in the conventional charger controllers. However, this output cannot feed directly the inverter due to low current capacity. Instead, it is used to activate a relay and turn on/off the inverter and, therefore, the SFC [2].

The solar charger controller used to test this functionality (Epever MPPT IT4415ND) has four modes of operation (Manual, Light ON/OFF, light ON + Time and Time) which can be programmable. Manual operation is the user who turns the "Load Output" on the charge controller. Light ON/OFF, also known as Dusk-Dawn in cheaper charger controllers, turn on the load output when there is no more light and turn it off only when the light comes back. The working behavior of the Power ON/OFF mode is described in Fig. 3.10 [2].

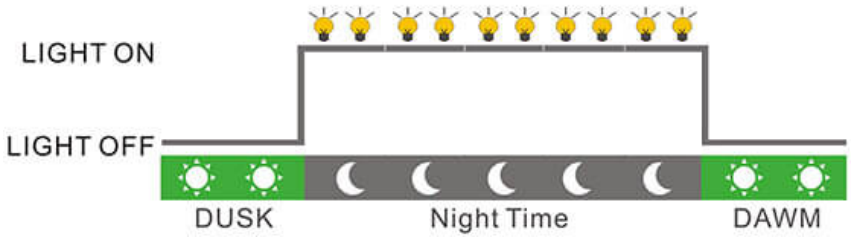

Figure 3.10: Working behavior of the charge controller in the "Power ON/OFF" mode. Adapted from [19].

Light ON + Time mode turns the load output on a set time after the sun goes down and before the sun rises as shown in Fig. 3.11. Time mode turns on and off the load in programmed by user hours.

Light ON/OFF was the mode chosen for the application. By default, it turns the "Load Output" OFF during the day and turns it ON during the night. Since it has reversed logic, a relay with 2 normally closed switches was used to ensure the desired logic and turn OFF the battery inverter and the voltage divider during the night and, therefore, reduce the self-consumption, as described before. An example of this type of connection is shown in Fig. 3.12 [2].

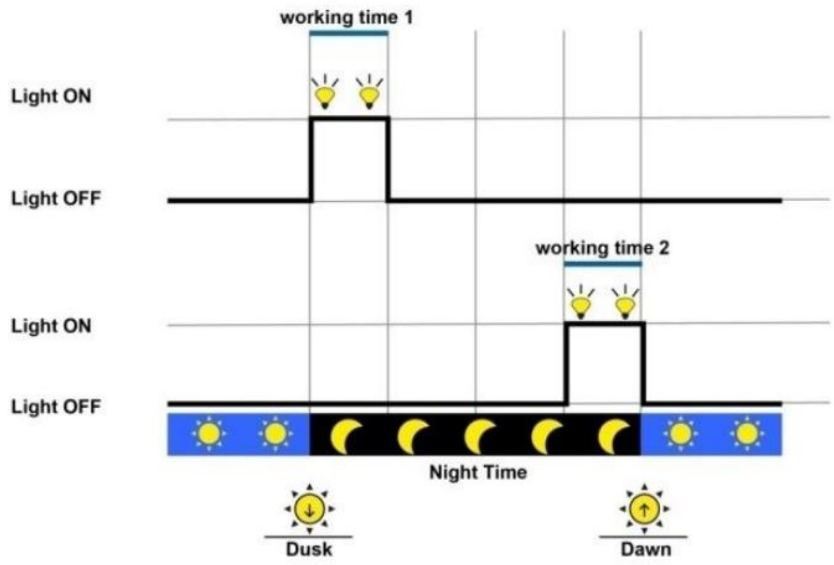

Figure 3.11: Working behavior of the charge controller in the "Power ON + Timer" mode [20].

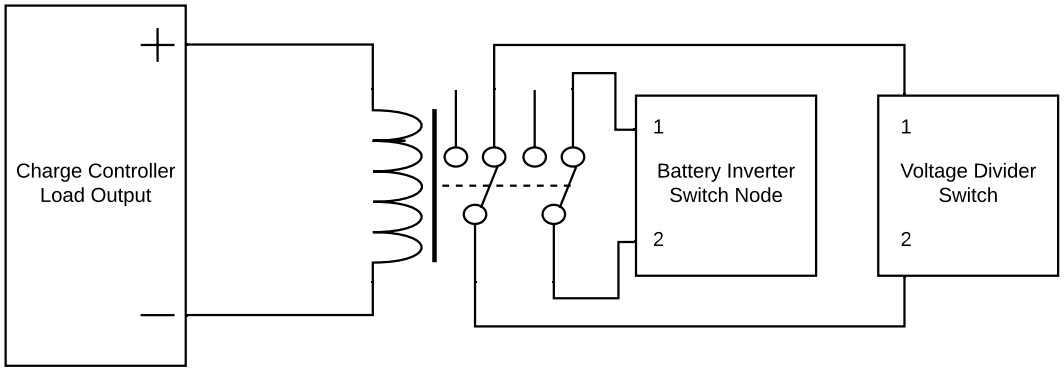

Figure 3.12: Example of the conection with the relay to turn off the battery inverter during the night.

Although that in cheaper charge controllers normally the Light ON/OFF (Dusk-Dawn) mode does not permit any kind of parametrization, this one specifically does. The settings of the used charge controller let the user set the "Night Time Threshold Voltage", "Day Time Threshold Voltage" and "Delay Time". The "Night Time Threshold Voltage" is the voltage in the array of modules to be considered as night. The "Day Time Threshold Voltage" is the voltage in the array of modules to be considered a day. The "Delay Time" is the time that the voltage must attend the threshold to change the state.

One good voltage to be set as "Day Time Threshold Voltage" is the V_{oc} of the solar

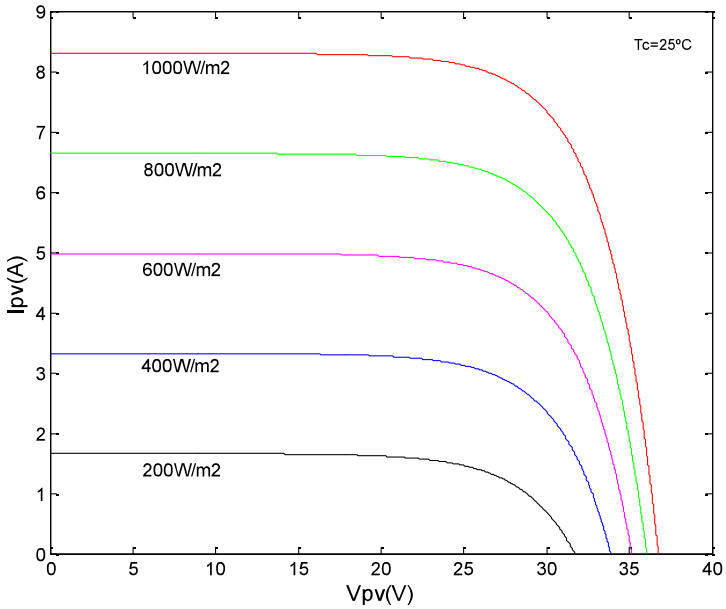

Figure 3.13: Example of how the irradiance affect the characteristic curve of a solar module [21].

module with a medium irradiance and a low temperature, for cases with more than 600 W/m^2 and temperatures below 25°C. This is a good point because it turns battery inverter on only when there is enough irradiance in the day and when the battery is completely full. A good voltage to be set as "Night Time Threshold Voltage" is the Maximum Power Point Voltage (V_{mpp}) of the solar module with a low irradiance and a medium temperature, like less than 400 W/m^2 and above 45°C. The way that the irradiance and temperature influence in the characteristic curves of the solar modules are shown in Fig. 3.13 and Fig. 3.14.

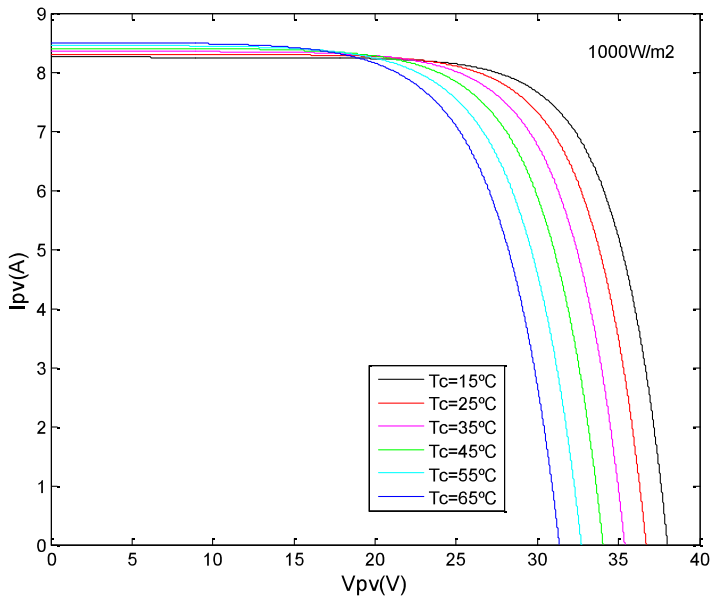

Figure 3.14: Example of how the temperature affect the characteristic curve of a solar module [21].

3.2 PVWPS based on SFCs without batteries

A more compact approach, that avoids the use of batteries, is presented in Fig. 3.15. This approach replaces the charge controller, batteries and the inverter by a DC-DC power converter. The DC-DC Converter boosts the voltage directly from the PV modules to the DC Link of the SFC. This strategy is not "plug and play" as the previous one. The development of this approach is not possible for most of the small companies unless they have a cooperation with a research or development institution. This work is an example of this cooperation [2].

3.2.1 DC-DC Converter

There are many DC-DC converter topologies, like boost, SEPIC/Cuk, flyback, forward or push-pull. The boost was chosen due to the simplicity of the topology. The boost converter topology is shown in Fig. 3.16. The boost has an inductor, a capacitor, a switching device (as a MOSFET or IGBT) and a diode. Of course this simplicity comes with a price: the input is not isolated from the output. For this application, the lack of

isolation is not a problem because even if something goes wrong, the maximum voltage in the output is approximately the open circuit voltage of the array, and the current is the short-circuit current (no more than 9 A).

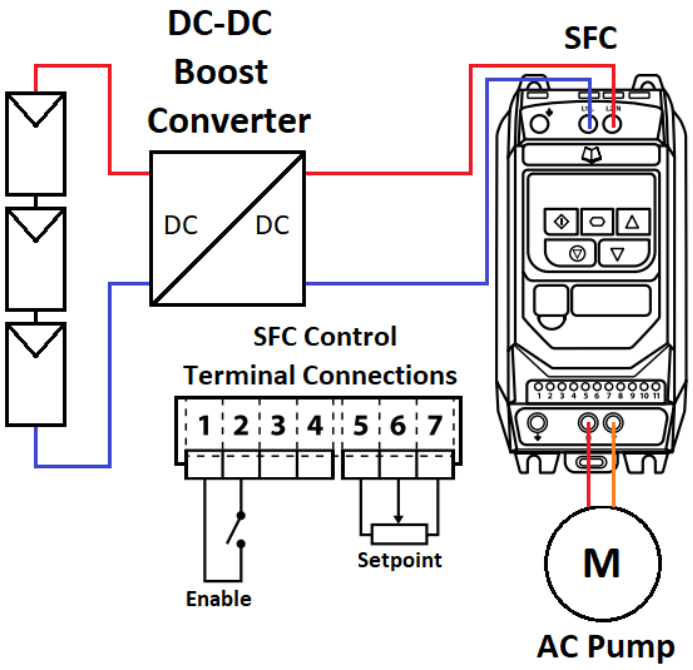

Figure 3.15: PVWPS for low power applications with the control conections, using a power boost converter and a SFC.

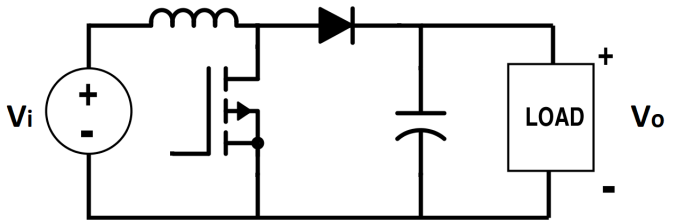

Figure 3.16: Topology of the boost converter.

Working in the continuous current mode, that is, the current in the inductor never goes to zero, it has 2 working stages. In the stage in which the switch is closed, represented in Fig. 3.17, the inductor gets charged and the load is fed with the capacitors. In the stage in which the switch is open, represented in Fig. 3.18, the load and the capacitor are fed by the discharging inductor.

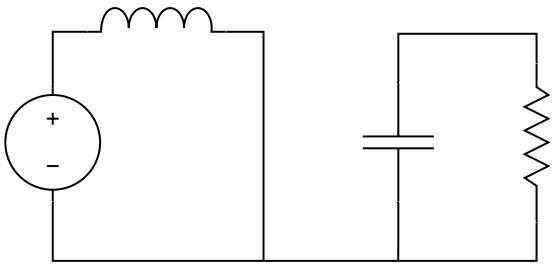

Figure 3.17: Stage one of the boost converter in continuous mode (switch ON)

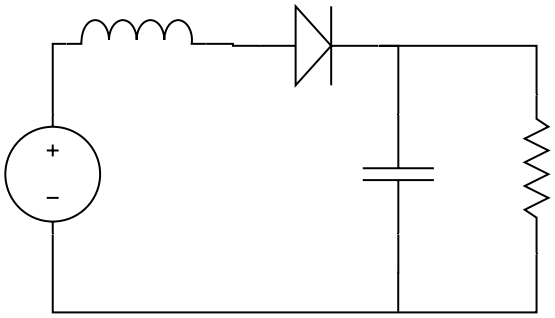

Figure 3.18: Stage two of the boost converter in continuous mode (switch OFF)

The major working principle of the boost converter in continuous mode is that the energy absorbed by the inductor in stage one is the same that discharges in the circuit. Therefore, the area 1 and area 2 of Fig. 3.20 is the same. With this information, it is possible to write Equation 3.3.

$$V_i T_{on} + (V_i - V_o) T_{off} = 0 \tag{3.3}$$

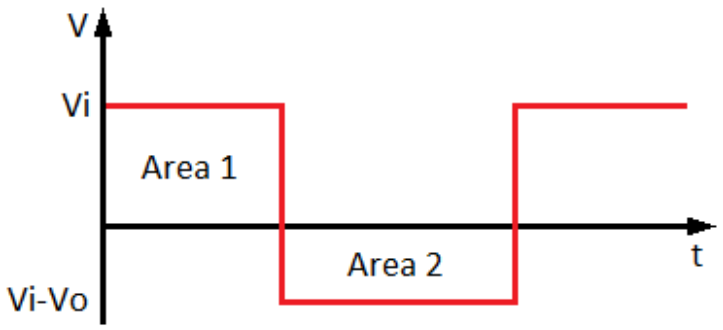

Figure 3.19: Voltage in the inductor of the boost converter in continuous mode vs time.

In the Equation 3.3, T_{on} represents the time that the switch is closed, represented by area 1 in Fig. 3.19. T_{off} represents the time that the switch is open, represented by area 2. Calling the total time T_s and dividing all for it the Equation 3.4 is given.

$$V_i \frac{T_{on}}{T_s} + (V_i - V_o)\frac{T_{off}}{T_s} = 0 \tag{3.4}$$

With simple algebra operations, the equations 3.4 and 3.5 result in Equation 3.6, that is the main equation of the boost converter in continuous mode.

$$T_{off} = T_s - T_{on} = T_s - DT_s = T_s(1 - D) \tag{3.5}$$

$$\frac{V_o}{V_i} = \frac{T_s}{T_{off}} = \frac{1}{1 - D} \tag{3.6}$$

Using Equation 3.6 it is possible to get the blue line of the graph represented in Fig. 3.20. Although this equation does not consider intrinsic losses to real elements. A more realistic representation is the orange one, where after some point of duty cycle the power losses start to become significant. From this graph it is also possible to notice that in the boost converter the smallest voltage in the output V_o is the input voltage V_i.

The boost converter was designed to work in a continuous mode of conduction. The equations to design the capacitor and the inductor are described in 3.7 and 3.8, respectively. The equations were adapted from [22].

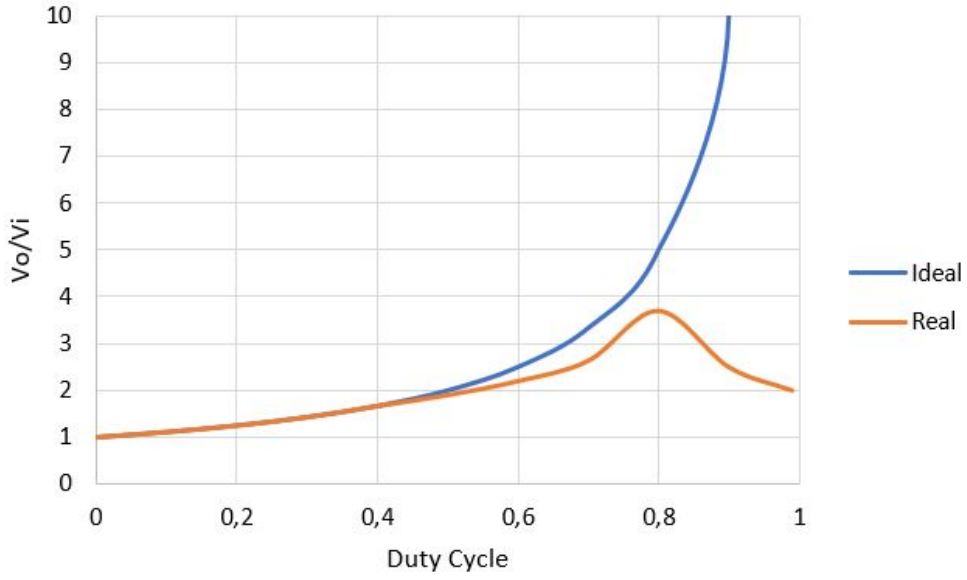

Figure 3.20: $\frac{V_o}{V_i}$ x Duty cycle ideal and real in a boost converter.

$$C = \frac{I_o D}{f_s \Delta V_o} \tag{3.7}$$

$$L = \frac{V_i D}{f_s (\Delta I_L)} \tag{3.8}$$

Each part of the formula is described next. I_o= current at the output; D = duty cycle; f_s = switching frequency; ΔV_o = ripple of the output voltage; V_i = input voltage; ΔI_L = ripple of the in inductor current.

The considered input voltage (V_i) is around 118 V, which is the voltage at the MPP of the four PV modules string with the modules Fluitecnik fts 220p, and the output voltage (V_o) chosen to the design is 310 V, which is an intermediate voltage in the DC-link of the SFC. The output power considered is 800 W. Due to the application voltage, the switch is an IGBT, and due to that, the switching frequency is 25 kHz. To discover the duty cycle the equation 3.9 is needed. Substituting the values on the equation and manipulating the duty cycle of 0,62 is discovered. The variation in inductor current and output voltage considered was 50% and 2%, respectively.

Table 3.3: Components Used in the Boost Converter

Type of Component	**Choosed Component**
Inductor	2 mH Ferrite Inductor
Capacitor	Equivalent 150 µF-500V Electrolytic Capacitor
Diode	Schottky DSEI 30-10 AR
Switch	IGBT G4PH50KD

$$\frac{V_o}{E} = \frac{1}{1-k} \tag{3.9}$$

With the available information it is possible to substitute the values in the equations 3.7 and 3.8, arriving in a minimum inductance and capacitance of 2.27 mH and 27 μF, respectively. The maximum current at the IGBT and inductor can be calculated using the equation 3.10, arriving at approximately 7.5 A. When the IGBT is open the voltage on it is the input voltage (E), being closed is the capacitor voltage (V_o), how is applied, therefore the maximum voltage in the IGBT will be V_o.

$$I_M = \frac{I_o}{1-D} + \frac{DV_o}{2Lf_s} \tag{3.10}$$

The final list of components, taking into consideration the functioning requirements, is shown in table 3.3.

However, the inductor is smaller than it should for a matter of disponibility of ferrite cores and enameled copper wire in the laboratory of this work. As a matter of fact, all these components were chosen because they were available in the laboratory, respecting the calculated values.

It is intended to keep this approach, as much as possible, feasible, simple and cost-effective for small companies. Therefore, the boost controller was designed using a well-known PWM controller: the IC TL494. The TL494 diagram is shown in Fig. 3.21 [2].

The TL494 Pulse width modulation (PWM) Controller integrates all the functions that are needed for this application. It contains two error amplifiers, which can be used

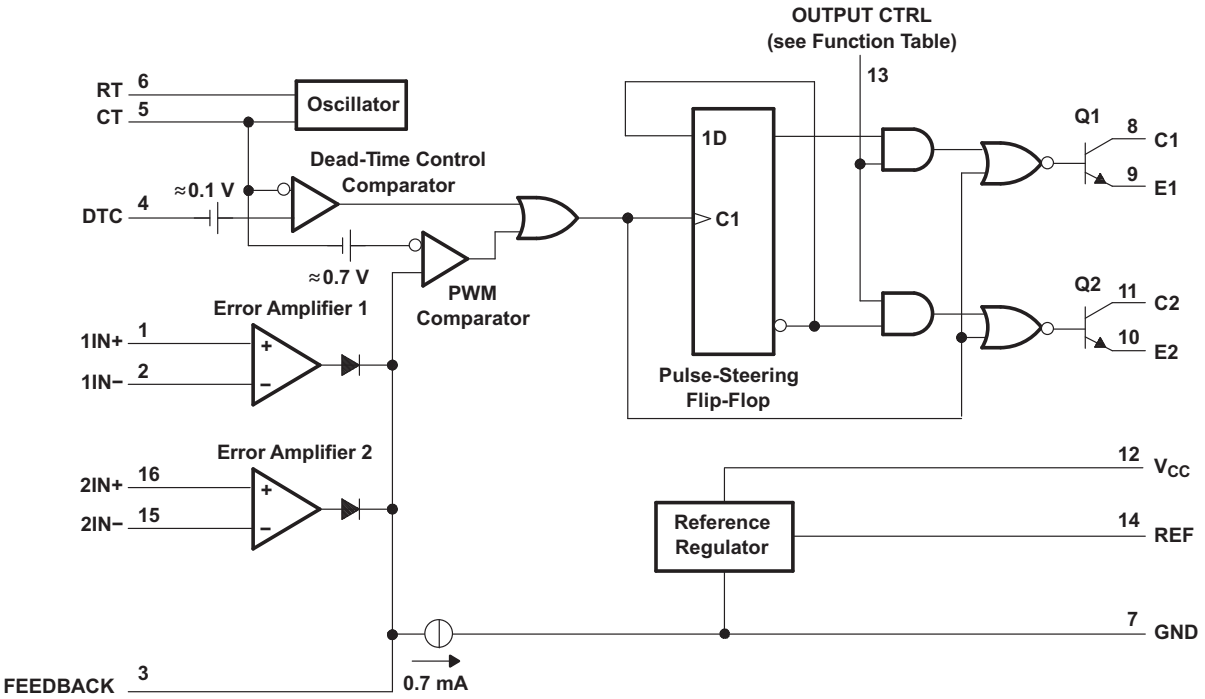

Figure 3.21: TL494 PWM Controller [23].

for the two desired control functions. The first control function extracts the maximum power of the PV modules by defining a suitable setpoint, which must be equal to the expected MPP voltage, for the higher irradiance levels, in summer. Thus, it is ensured that the pump will work close to the MPP in the summer. However, the system will not work with the maximum power efficiency most of the time, but in most cases, it is in the summer that the water is most needed [7]. Secondly, the controller must protect the SFC by limiting the maximum DC voltage applied to the SFC. This limit was set to 350 V. The absolute maximum voltage is given by maximum amplitude of the input AC voltage. In this case, it is 373 V for this specific single-phase SFC [2].

The boost converter and a schematic of the control circuit are shown in Fig. 3.22.

The control function that extracts the maximum power is done by the error amplifier 1 of the TL494. A voltage divider dimensioned to give no more than 5 V is connected in parallel to the PV array. The voltage given by the PV voltage divider goes to the inverting input (–). To the noninverting input (+) is connected a voltage divider, with a

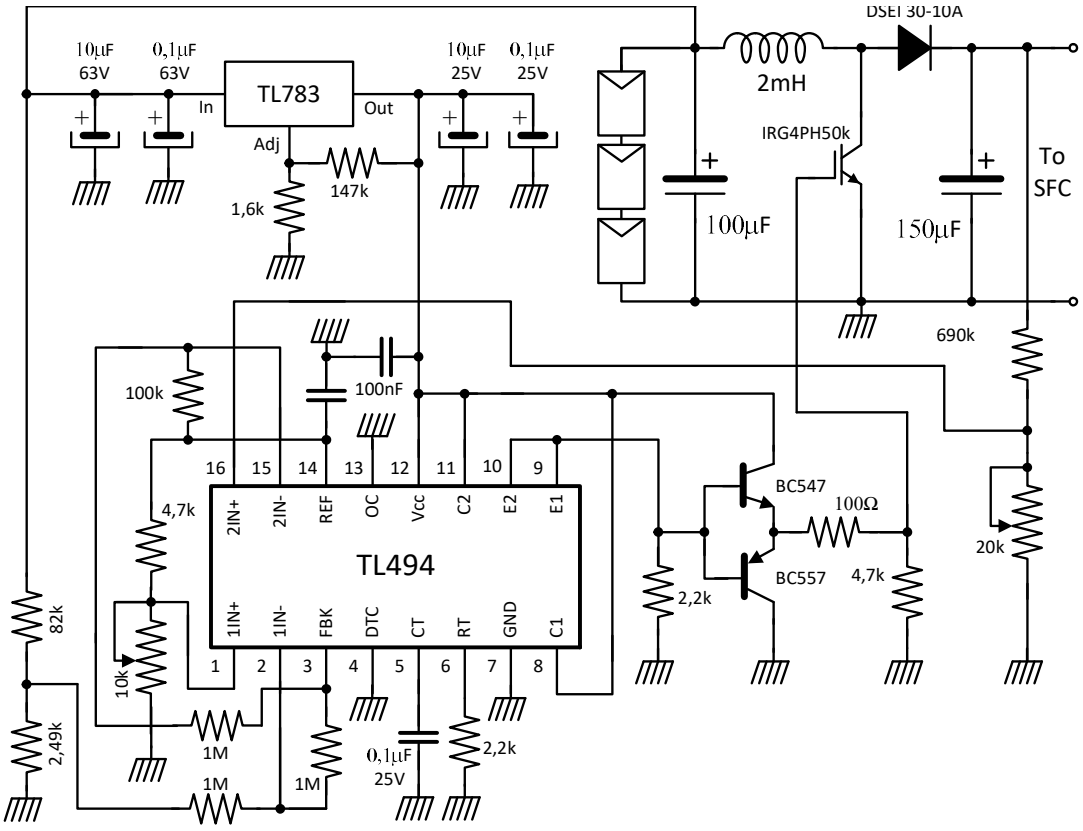

Figure 3.22: Boost converter and the schematic of the control circuit.

potentiometer, connected to the TL494 internal power supply of 5 V. The potentiometer is set to have at the output of the PV modules the MPP voltage in the summer, drawing near maximum energy in summer. This adjust is made by the PWM controller changing the duty cycle.

The control function that limits the output voltage of the boost converter is done by the error amplifier 2 of the TL494. A voltage divider with a potentiometer is dimensioned to give 5 V when the output has 350 V. This voltage divider is connected in parallel to the load output. The voltage given by the PV voltage divider goes to the noninverting input (+). To the inverting input (-) is connected to the TL494 internal power supply of 5 V. The potentiometer is set to adjust the maximum desired output voltage. This adjust is made by the PWM controller changing the duty cycle.

The characteristic that permits these two controls to work in parallel is that the smallest error overcomes the bigger, so the controls were made to the protection function is always be the principal. It means that if the output voltage reaches 350 V, automatically the boost takes out the functioning point of the MPP in summer and adjusts the duty cycle to the voltage do not go higher.

The operation of the SFC is carried on in order to keep the speed proportional to the radiation, i.e., to the power provided by the boost converter. For this purpose, it is used the macro PID, available in all SFC, with closed loop control of the pump's speed, and using the DC-Link voltage of the SFC as a process variable (feedback signal). The setpoint is fixed and within the input range of amplitude, as if it was connected to the main grid. The block diagram is in Fig 3.23 [2].

In this way, when the voltage goes under or higher than the voltage setpoint, the speed of the pump decreases or increases, respectively, in order to keep the DC-Link voltage equal to the setpoint.

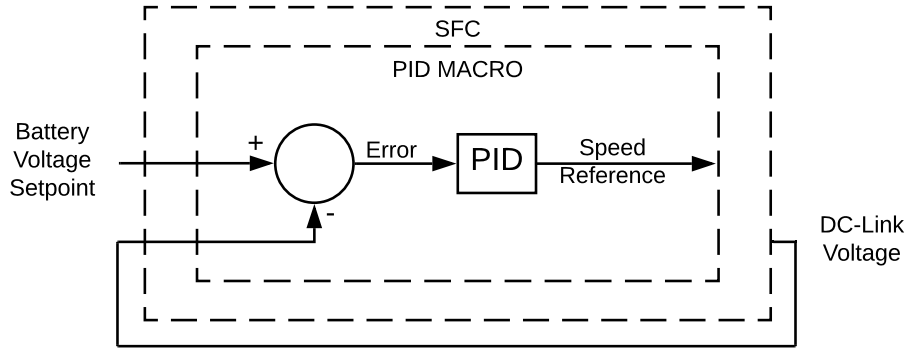

Figure 3.23: Control scheme of the SFC using the macro PID, and the DC-Link voltage as process variable, to control the speed of the pump.

3.3 Challenges on PVWPS Based on SFCs (With or Without Batteries)

Parametrization for Experiments with batteries

In the previous subsections some parameters of the SFC were explained and what they are used for, although they are not all. All the parameters and the reason why they were used, are described in this section.

In order to connect the water pump and drive it with the SFC the motor-related parameters must be set. The most important ones are those that refer to the motor nameplate values, such as voltage, current, frequency and speed. These can be set using the following parameters in the Invertek SFC:

- P-07 - Motor Rated Voltage (volts)
- P-08 - Motor Rated Current (amperes)
- P-09 - Motor Rated Frequency (Hertz)
- P-13 - Operating Mode Select (type of application)

Two other basic parameters can also be set: the minimum and maximum output frequency, and acceleration and deceleration ramp times. These can be set using the following parameters:

- P-01 - Maximum Frequency / Speed Limit (Hz or RPM)
- P-02 - Minimum Frequency / Speed Limit (Hz or RPM)
- P-03 - Acceleration Ramp Time (s)
- P-04 - Deceleration Ramp Time (s)

These two first parameters are useful to limit the power delivered to the motor to the peak power that can be obtained with the photovoltaic array. Besides that, the minimum frequency parameters can be set and, together with the PI control, can be used to, in case the pump is being driven at the minimum speed for a definite amount of time, a sign that the power generated by the solar panels is insufficient, the SFC can turn the pump off.

The Invertek SFC has a set of advanced parameters, which address features like the V/F control or the PI control. To obtain access and set advanced parameters, that is, parameters P-14 to P-60, the parameter P-14 must be set with a value equal to 101.

Some parameters configure the way inputs and outputs work during operation. These parameters are especially important to configure the signals in the PI control method and are listed as follows:

- P-12 - Primary Command Source
  - Defines the control mode used, which defines how the motor will be controlled. The modes can be Terminal Control, Uni-directional Keypad Control, Bi-directional Keypad Control, Modbus Network Control, Modbus Network Control, PI Control, PI Analog Summation Control, CAN Control or Slave Mode.
- P-15 - Digital Input Function Select
  - Defines the function of the inputs depending parameter P-12. This functions, in the case of the PI control, is shown in Fig. 3.24.
- P-16 - Analog Input 1 Signal Format

P-15	DI1		DI2		DI3 / AI2		DI4 / AI1		Diagram
	0	1	0	1	0	1	0	1	
0	STOP	ENABLE	PI REF	P-20 REF	AI2		AI1		4
1	STOP	ENABLE	PI REF	AI1 REF	AI2 (PI FB)		AI1		4
3, 7	STOP	ENABLE	PI REF	P-20	E-TRIP	OK	AI1 (PI FB)		3
4	(NO)	START	(NC)	STOP	AI2 (PI FB)		AI1		12
5	(NO)	START	(NC)	STOP	PI REF	P-20 REF	AI1 (PI FB)		5
6	(NO)	START	(NC)	STOP	E-TRIP	OK	AI1 (PI FB)		
8	STOP	RUN	FWD ↻	REV ↺	AI2 (PI FB)		AI1		4
14	STOP	RUN	-	-	E-TRIP	OK	AI1 (PI FB)		16
15	STOP	RUN	P-23 REF	PI REF	Fire Mode		AI1 (PI FB)		1
16	STOP	RUN	P-23 REF	P-21 REF	Fire Mode		AI1 (PI FB)		1
17	STOP	RUN	P-21 REF	P-23 REF	Fire Mode		AI1 (PI FB)		1
18	STOP	RUN	AI1 REF	PI REF	Fire Mode		AI1 (PI FB)		1
2,9,10,11,12,13 = 0									
NOTE	**P1 Setpoint source is selected by P-44 (default is fixed value in P-45, A11 may also be selected).** **P1 Feedback source is selected by P-46 (default is A12, other options may be selected).**								

Figure 3.24: Macro functions of PI control mode [18].

  - Defines the format accepted by the terminal 6 (analog input 1). The possible options are 0-10 V unipolar or bidirectional operation, 0-20 mA and 4-20 mA. These can also be reversed to operate with ranges such as 10-0V or 20-4 mA, for example.

- P-25 - Analog Output Function Select

  - Defines the functions of the analog output terminal, offering two choices, either digital or analog. In the digital mode, one can select to output digital states such as if the drive is running, if the drive tripped, etc. If the output is chosen to be analog, the output signal will reflect the chosen variable in a range from 0 to 10 V. The variables that can be selected are: the motor speed, motor current, motor power or load current.

- P-47 - Analog Input 2 Signal Format

  - Defines the format accepted by the terminal 4 (analog input 2). The possible options are 0-10 V, 0-20 mA and 4-20 mA. These can also be reversed to operate with ranges like 20-0 mA or 20-4 mA, for example. This analog input can also be used with a motor thermistor.

Using the PI control may require the setting of a few parameters, as listed in the following list, containing a brief explanation on the listed parameters as well:

- P-35 - Analog Input 1 Scaling
  - Parameter to set the factor that multiplies the analog input signal level.
- P-39 - Analog Input 1 Offset
  - Parameter to set an offset to the applied analog input signal.
- P-41 - PI Controller Proportional Gain
  - Parameter to set the proportional gain of the PI control.
- P-42 - PI Controller Integral Time
  - Parameter to set the integral time of the PI Control.
- P-43 - PI Controller Operating Mode
  - Parameter to select how the PI control will work. There are four modes, direct operation, inverse operation, direct operation with wake at full speed and inverse operation with wake at full speed. Direct operation means that, when the feedback signal drops, the motor speed increases and inverse operation that, when the feedback signal drops, the motor speed drops as well. The wake at full speed means that, when restarting from standby, the PI output is set to 100%.
- P-44 - PI Reference (Setpoint) Source Select
  - Parameter to set whether the PI reference source will be analog or digital. If analog, the reference is given by analog input 1.
- P-46 - PI Feedback Source Select

  - Parameter to set what will be the feedback source. The feedback can be the Analog Input 1 or 2, Motor Current, DC Bus Voltage, Analog 1 – Analog 2 or the Largest (Analog 1, Analog 2).

- P-48 - Standby Mode Timer
  - Parameter to set how much time the SFC works with the minimum frequency before entering in standby mode.

- P-49 - PI Control Wake Up Error Level
  - Parameter to set the error of the PI to the SFC resumes normal operation after entering standby mode. The error is the difference between the setpoint and feedback signal. This allows the SFC to only come back when there are enough conditions to it.

To permit the operation after a trip of the SFC for a full tank or other condition and the SFC starts alone after energized there is a specific parameter:

- P-30 - Start Mode, Automatic Restart, Fire Mode Operation
  - Parameter to set if the drive should start automatically if the enable input is latched during power on and how the automatic restart should work. The automatic restart delay is limited to 5 attempts with a 20 seconds interval.

Full Tank and Empty Well Protections

There are SFCs, such as ABB ACS355, which have undercurrent and overload protection. These protections would be enough with a simple buoy valve in the tank, as shown in Fig. 3.25.

If the pump works with an empty well it will work with a low current, tripping the undercurrent protection. Furthermore, if the pump work and the tank are full (with a buoy valve) the pressure in the tube will rise, making the work of the pump difficult and the current rise, tripping the overload protection.

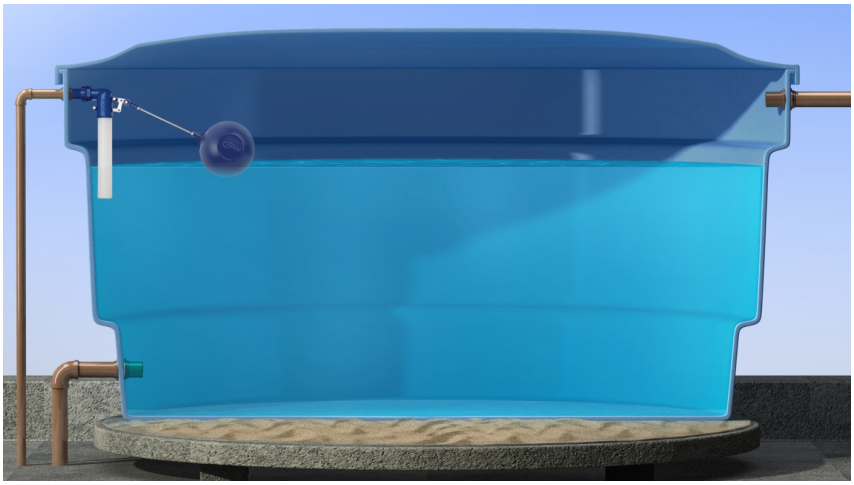

Figure 3.25: Exemple of a buoy valve instaled [24].

However, the SFC used, the Invertek Optidrive E3, just have the overload protection, as shown in Fig. 3.26. This overload protection trips when the current is higher than the value set as the rated current for an extended period of time (like 60 seconds). It is also possible to use a motor thermistor to trip the overload protection when the motor reaches a high temperature.

Motor Thermal Overload Protection

Internal Thermal Overload Protection

The drive has an in-built motor thermal overload function; this is in the form of an "I.t-trP" trip after delivering >100% of the value set in P-08 for a sustained period of time (e.g. 150% for 60 seconds).

Motor Thermistor Connection

Where a motor thermistor is to be used, it should be connected as follows:

Control Terminal Strip	Additional Information
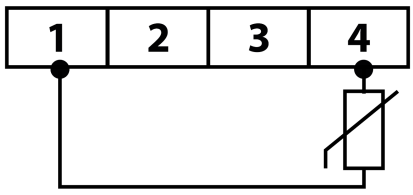	Compatible Thermistor: PTC Type, 2.5kΩ trip level. ▪ Use a setting of P-15 that has Input 3 function as External Trip, e.g. P-15 = 3. Refer to section 7. Analog and Digital Input Macro Configurations on page 31 for further details. ▪ Set P-47 = "PtC-tH"

Figure 3.26: Overload protection in the Invertek Optidrive E3. Adapted from [18].

As the SFC does not have undercurrent protection it is necessary to have an external sensor, like the electrical buoy shown in Fig. 3.27.

Figure 3.27: Exemple of a electrical buoy.

Although the protection will work, if the overload protection is activated probably the pump will come back to work only in the next day because probably the limit of 5 attempts with a 20 second interval in P-30 is not enough to empty the tank enough for the pump run normally. On the other hand, the protection of empty well is just an "enable" switch, so if the level of water return to good conditions to the pump it will resume normal operation.

Chapter 4

Validation with Hardware

The validation of the proposed solutions for low power PVWPS was reached using the components described in the following subsections. These components were chosen because they were available in the laboratory or made available by the partner company.

The results were obtained using the single-phase input/output SFC Invertek Optidrive E3 and the PV modules FTS-220P from Fluitecnik. By using a single-phase input, it is possible to reduce the number of PV modules needed to generate the DC voltage required by the SFC. On the other hand, the single-phase output enables the use of the most common AC pumps for low power levels (up to several hundreds of W) [2].

4.1 Tests

4.1.1 PVWPS Based on SFCs with Batteries

To validate this approach the equipment is described in Table 4.1. The pumps, PV modules, battery inverters, charge controllers, standard frequency converter and batteries are shown in Fig. 4.1, 4.2, 4.3, 4.4, 4.5 and 4.6, respectively. These equipment were used in a total of 7 tests, which the results are explained in the sequence of section and summarized in the Table 4.2.

Table 4.1: Equipment used in the experimental platform.

Component	Equipment Used
Photovoltaic Module	REC 275PE 275W
Photovoltaic Module	Fluitecnik FTS-220P 220W
Charge Controller	Steca PR2020 PWM
Charge Controller	Epever IT4415ND MPPT
Battery	Ultracell UCG 20-12
Battery	Sonnenschein S12/17 G5
Battery	MasterBat MBG100Ah-12V
Battery Inverter	Cotek 12VDC-230VAC-600W Pure Sine
Battery Inverter	Epever SHI 300 24V-230V-300W Pure Sine
Battery Inverter	Carspa 12VDC-230VAC-1000W Modified Sine
Battery Inverter	HQ 24VDC-230VAC-600W Modified Sine
Battery Inverter	Epever SHI 3000 48V-230V-3000W Pure Sine
Standard Frequency Converter	Invertek Optidrive E3 1HP Single-Phase Input/Output
Pump	Sterwins 750 DW-3 1HP
Pump	Pentax CR100/00/1 1HP

Table 4.2: Test Summary.

Test	Successful
A	No
B	No
C	No
D	Yes
E	Yes
F	Yes
G	Yes

For tests A, B, C, D, and E the closed loop control used was the first presented in 3.1.1. The first closed loop control uses the speed of the pump as the feedback and the battery voltage as the setpoint. The tests F and G used the second closed loop control presented in 3.1.1. The second closed loop control uses the battery voltage as feedback and the battery voltage reference as the setpoint.

Only the tests F and G used the charge controller parametrization to turn off the inverter at night.

The parameters presented in Table 4.3 are common to all experiments. The parameter of minimum frequency (P-02) was obtained on experiments that concluded that in 30 Hz the pump is out of the initial inertia. The PI parameters (P-41 and P-42) were set by experimentation.

Table 4.3 contains the basic parameters to all tests with batteries.

Figure 4.1: Pumps used in the tests, (A) Pentax CR100/00/1 1HP, (B) Sterwins 750 DW-3 1HP.

(A) (B)

Figure 4.2: PV Modules used in the tests, (A) REC 275PE 275W, (B) Fluitecnik FTS-220P 220W.

(A) (B) (C) (D) (E)

Figure 4.3: Battery inverters used in the tests, (A) Cotek 12VDC-230VAC-600W Pure Sine, (B) HQ 24VDC-230VAC-600W Modified Sine, (C) Carspa 12VDC-230VAC-1000W Modified Sine, (D) Epever SHI 3000 48V-230V-3000W Pure Sine, (E) Epever SHI 3000 48V-230V-3000W Pure Sine.

(A) (B)

Figure 4.4: Charge controllers used in the tests, (A) Epever IT4415ND MPPT, (B) Steca PR2020 PWM.

Figure 4.5: SFC used in the tests: Invertek Optidrive E3 1HP Single-Phase Input/Output.

Figure 4.6: Batteries used in the tests, (A) MasterBat MBG100Ah-12V, (B) Ultracell UCG 20-12, (C) Sonnenschein S12/17 G5.

Table 4.3: Basic parameters attributed values.

Parameter	Description	Attributed value
P-01	Maximum Frequency	30 Hz
P-02	Minimum Frequency	50 Hz
P-03	Acceleration Ramp Time	5 s
P-04	Deceleration Ramp Time	5 s
P-07	Motor Rated Voltage	230 V
P-08	Motor Rated Current	5.4 A
P-09	Motor Rated Frequency	50 Hz
P-10	Motor Rated Frequency	2800 RPM
P-12	Primary Command Source	5 - PI Control
P-15	Digital Input Function Select	0
P-16	Analog Input 1 Signal Format	U 0-10 - Uni-polar 0-10 Volt Signal
P-30	Start Mode, Automatic Restart, ...	Auto-5
P-41	PI Controller Proportional Gain	1
P-42	PI Controller Integral Time	2
P-44	PI Setpoint Source Select	1 - Analog Input 1 Setpoint
P-46	PI Feedback Source Select	0 - Analog Input 2
P-47	Analog Input 2 Signal Format	U - 0 to 10 Volt Signal
P-48	Standby Mode Timer	10 seconds

For tests A, B, C, D, and E the parameters presented in Table 4.4 were used. The P-35 and P-39 were set according to the test and voltage of the voltage divider.

Table 4.4: Exclusive parameters in tests A, B, C, D and E.

Parameter	Description	Attributed value
P-25	Analog Output Function Select	8 - Output Frequency
P-35	Analog Input 1 Scaling	-
P-39	Analog Input 1 Offset	-
P-43	PI Controller Operating Mode	0 - Direct Operation
P-49	PI Control Wake Up Error Level	48%

To tests F and G the parameters presented in 4.5 were used.

Table 4.5: Exclusive parameters in tests F and G.

Parameter	Description	Attributed value
P-43	PI Controller Operating Mode	1 - Inverse Operation
P-49	PI Control Wake Up Error Level	7%

Test A

To this validation was used one battery Sonnenschein S12/17 G5, two REC 275PE 275W PV modules connected in parallel, the Steca PR2020 PWM charge controller, the Cotek 12VDC-230VAC-600W pure sinewave battery inverter and the Pentax CR100/00/1 1HP pump.

During the sunny hours, the system was assembled as a whole and made dependent only on the power provided by the PV modules. In this test, only one 12V battery was connected to the Steca PR2020 MPPT charger. The power required by the pump due to the inrush current was too high. This generates a high voltage drop on the internal resistance of the battery and consequently a voltage lower than the minimum required by

the Cotek inverter to operate properly. Another important factor is that 2 PV modules and a 20 A in 12 V charge controller are not ideal for this application. These two PV modules together have 550 Wp and the charge controller only supply 240 W (12 V x 20 A). Taking into account that the pump has approximately 750 W, all the rest of the energy the battery has to supply. However after the pump starts the energy would be suitable for lower speeds, nevertheless it could not start.

As an outcome, the pump was unable to overcome the inertia before the SFC and inverter reported low voltage alerts and shut the system down.

Test B

To this validation two batteries Sonnenschein S12/17 G5 were connected in series (24 V equivalent), two REC 275PE 275W PV modules connected in parallel, the Steca PR2020 PWM charge controller, the Epever SHI 300 24V-230V-300W pure sinewave battery inverter and the Pentax CR100/00/1 1HP pump.

During the sunny hours, the system was assembled as a whole and made dependent only on the power provided by the PV modules. In this test, an arrangement with 2 batteries connected in series (24 V equivalent), was connected to the Steca PR2020 MPPT charger. The results were the same as in test A. The inrush current of the pump was too high to the system support, even that now the charger controller can deliver 480 W (24 V x 20 A). However, 2 PV modules and a 20 A in 24 V charge controller are not ideal for this application. These two PV modules together have 550 Wp, the charge controller only supplies 480 W to a pump that has almost 750 W, letting all the rest to the battery absorb. However, after the pump starts the energy would be enough for lower speeds, but it could not start.

As an outcome, the pump was unable to overcome the inertia before the SFC and inverter reported low voltage alerts and shut the system down.

Test C

Instead of connecting two batteries of 12V in series this test used two, three and four batteries Sonnenschein S12/17 G5 connected in parallel, two REC 275PE 275W PV modules connected in parallel, the Steca PR2020 PWM charge controller, the Cotek 12VDC-230VAC-600W pure sinewave battery inverter and the Pentax CR100/00/1 1HP pump. The platform of this test is shown in Fig. 4.7.

Figure 4.7: Platform of test C.

During the sunny hours, the system was assembled as a whole and made dependent only on the power provided by the PV modules. In this test only up to four batteries

in parallel (12 V equivalent) were connected to the Steca PR2020 MPPT charger. The power required by the pump due to the inrush current was too high. This generates a high voltage drop on the internal resistance of the battery and consequently a voltage lower than the minimum required by the Cotek inverter to function properly. Another important factor is that 2 PV modules and a 20 A in 12 V charge controller are not ideal for this application. These two PV modules together have 550 Wp and the charge controller only supply 240 W (12 V x 20 A). Taking into account that the pump has approximately 750 W, the rest of the energy the battery has to supply. However after the pump starts the energy would be enough for lower speeds, but it could not start.

As an outcome, the pump was unable to overcome the inertia before the SFC and inverter reported low voltage alerts and shut the system down.

Test D

For this validation was used one battery Sonnenschein S12/17 G5, two REC 275PE 275W PV modules connected in parallel, the Steca PR2020 PWM charge controller, the Cotek 12VDC-230VAC-600W pure sinewave battery inverter and the Sterwins 750 DW-3 1HP pump.

During the sunny hours, the system was assembled as a whole and made dependent only on the power provided by the PV modules. In this test, only one 12V battery was connected to the Steca PR2020 MPPT charger. This pump requires less current to start, consequently, the current did not drop the voltage as it was happening with the Pentax pump. Even that only these 2 PV modules and a 20 A in 12 V charge controller are not ideal for this application, the system could work perfectly. How the modules were accessible it was possible to simulate shadows and verify that the PI was working as it should. When there was more irradiance the SFC increased the pump speed. When the irradiance went down or was a shadow made the SFC decreased the pump speed until the minimum frequency (P-02). When the pump stayed in the minimum frequency for the time set in P-48 the SFC entered standby mode, and it only went out of it when the PI error level (P-49) was bigger than the value set. An advantage of the system with

batteries is that the short-time drops in irradiance levels do not interrupt the operation of the pump.

As an outcome, this test was considered successful due to the fact that the control worked like it was expected and the approach was working effectively, validating the solution design.

Test E

To this validation the following equipment was used: one battery Ultracell UCG 20-12, two REC 275PE 275W PV modules connected in parallel, the Steca PR2020 PWM charge controller, the Carspa 12VDC-230VAC-1000W modified sinewave battery inverter and the Sterwins 750 DW-3 1HP pump. The platform of this test is shown in Fig. 4.8.

During the sunny hours, the system was assembled as a whole and made dependent only on the power provided by the PV modules. In this test, only one 12V battery was connected to the Steca PR2020 MPPT charger. This pump requires less current to start, consequently, the current did not drop the voltage as it was happening with the Pentax pump. Even that only these 2 PV modules and a 20 A in 12 V charge controller are not ideal for this application, the system could work perfectly. How the modules were accessible it was possible to simulate shadows and verify that the PI was working as it should. When there was more irradiance the SFC increased the pump speed. When the irradiance went down or was a shadow made the SFC decreased the pump speed until the minimum frequency (P-02). When the pump stayed in the minimum frequency for the time set in P-48 the SFC entered standby mode, and it only went out of it when the PI error level (P-49) was bigger than the value set. An advantage of the system with batteries is that the short-time drops in irradiance levels do not interrupt the operation of the pump.

Figure 4.8: Platform of test E.

As an outcome, this test was considered successful due to the fact that the control worked like it was expected and the approach was working completely, validating the solution design. This test validates also the possibility to supply energy to a SFC with a modified sinewave battery inverter, which has a significantly lower cost than a pure sinewave battery inverter.

Test F

To this validation four batteries Sonnenschein S12/17 G5 were used/connected in series (48 V equivalent), four Fluitecnik FTS-220P 220W PV modules connected two in series in parallel with the other two in series, the Epever IT4415ND MPPT charge controller, the Epever SHI 3000 48V-230V-3000W pure sinewave battery inverter and the Pentax CR100/00/1 1HP pump. The set of components used to validate this approach and collect the data presented in this work are shown in Fig. 4.9. This setup is very robust and sufficient for the application [2].

The charge controller was programmed with the Light ON/OFF operating mode. By default, it turns the load output OFF during the day and turns it ON during the night. Since it has reversed logic, a relay was used to ensure the desired logic and turn OFF the battery inverter during the night and, therefore, to reduce the self-consumption, as described before [2].

The system worked as it should. The charge controller turned off the battery inverter during the night and just turned on again when the sun was back. When there was more irradiance the SFC increased the pump speed. When the irradiance went down or was a shadow made the SFC decreased the pump speed until the minimum frequency (P-02). When the pump stayed in the minimum frequency for the time set in P-48 the SFC entered standby mode, and it only went out of it when the PI error level (P-49) was bigger than the value set. An advantage of the system with batteries is that the short-time drops in irradiance levels do not interrupt the operation of the pump.

Fig 4.10 presents one full day of operation. On this day, after some attempts of running, the pump starts working at 9:22 and stops at 16:31. These attempts are a consequence of

Figure 4.9: Experimental platform for low power applications based on the integration of a charge controller, a battery, a battery inverter and a SFC.

enough voltage provided by the battery charger due to the charging process. However, the current given by the irradiation level is not sufficient yet. These attempts (before 9:22) are not shown in Fig 4.10b) [2].

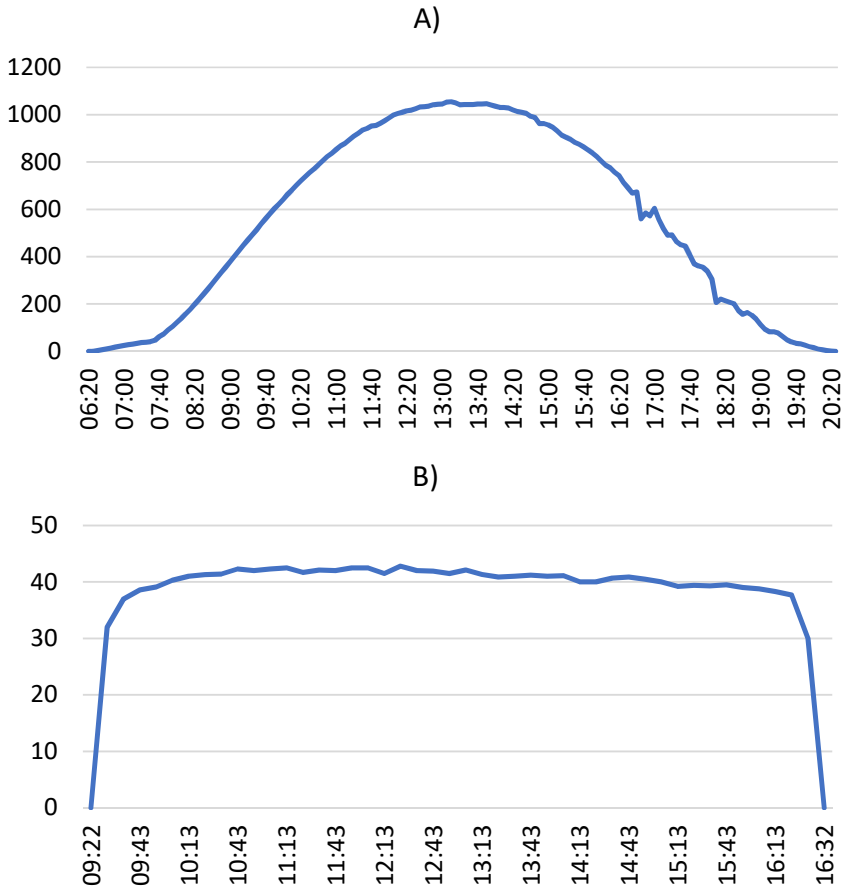

Figure 4.10: One day of operation of a low power applications based on the integration of a charge controller, a battery, a battery inverter and a SFC. A) Irradiation in Bragança vs hours (02/05/2019); B) Speed of the pump vs hours (02/05/2019).

Fig 4.11 presents one full day of operation. The pump stops two times in the morning due to the effect of the shadow produced by a 1.4 kW wind turbine, as shown in Fig. 4.12. On this day, after some attempts of running, the pump starts working at 9:58 and stops at 17:30. These attempts are a consequence of enough voltage provided by the battery charger due to the charging process. However, the current given by the irradiation level is not sufficient yet. These attempts (before 9:58) are not shown in Fig 4.11b). As can be seen from the analysis of Fig. 4.11, the presence of the battery mitigates the instability due to a sudden fall of irradiance. Indeed, the normal operation of the SFC (and pump) is not affected by a sudden lack of irradiance.

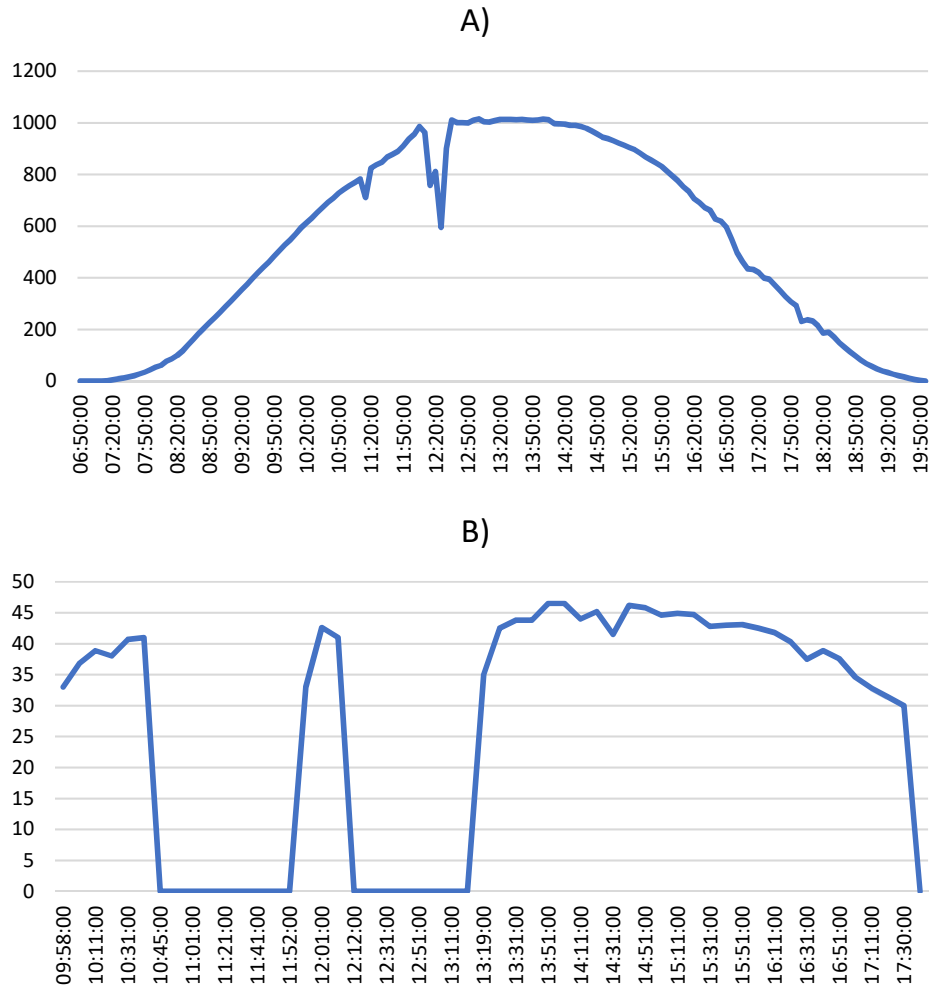

Figure 4.11: One day of operation of a low power applications based on the integration of a charge controller, a battery, a battery inverter and a SFC. A) Irradiation in Bragança vs hours (02/04/2019); B) Speed of the pump vs hours (02/04/2019).

As an outcome, this test was considered successful due to the fact that the control worked like it was expected and the approach was working completely, validating the solution design.

Test G

To this validation two batteries MasterBat MBG100Ah-12V were used in series (24 V equivalent), four Fluitecnik FTS-220P 220W PV modules connected two in series in parallel with the other two in series, the Epever IT4415ND MPPT charge controller, the

Figure 4.12: Shadow produced by a small wind turbine (02/04/2019 - 10:45).

HQ 24VDC-230VAC-600W modified sinewave battery inverter and the Pentax CR100/00/1 1HP pump. The set of components used to validate this approach and collect the data presented in this work are shown in Fig. 4.13. This setup is very robust and sufficient for the application.

The charge controller was programmed with the Light ON/OFF operating mode. By default, it turns the load output OFF during the day and turns it ON during the night. Since it has reversed logic, a relay was used to ensure the desired logic and turn OFF the battery inverter during the night and, therefore, to reduce the self-consumption, as described before.

The system worked as it should. The charge controller turned off the battery inverter during the night and just turned on again when the sun was back. When there was more irradiance the SFC increased the pump speed. When the irradiance went down or was a shadow made the SFC decreased the pump speed until the minimum frequency (P-02). When the pump stayed in the minimum frequency for the time set in P-48 the SFC entered standby mode, and it only went out of it when the PI error level (P-49) was bigger than the value set. An advantage of the system with batteries is that the short-time drops in irradiance levels do not interrupt the operation of the pump.

Figure 4.13: Experimental platform for low power applications based on the integration of a charge controller, a battery, a battery inverter and a SFC.

Figure 4.14 presents two hours of operation. These images show clearly that the pump is working proportional to the irradiance.

As an outcome, this test was considered successful due to the fact that the control worked like it was expected and the approach was working completely, validating the solution design. This test validates also the possibility to supply energy to a SFC with a modified sinewave battery inverter, which has a significantly lower cost than a pure sinewave battery inverter.

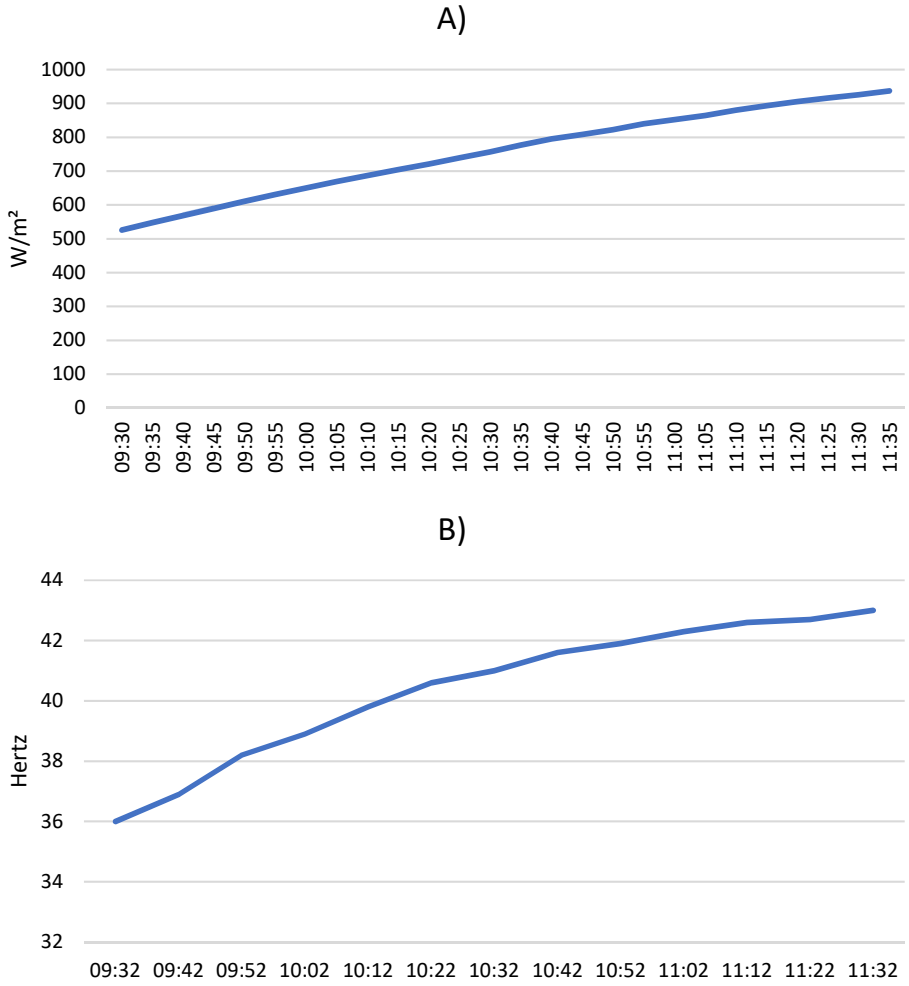

Figure 4.14: Two hours operation of a low power applications based on the integration of a charge controller, a battery, a battery inverter and a SFC. A) Irradiation in Bragança x hours (13/05/2019); B) Speed of the pump x hours (13/05/2019).

4.1.2 PVWPS based on SFCs without batteries

To this validation three Fluitecnik FTS-220P 220W PV modules were used connected in series, the boost converter and the 750 W single-phase submersible pump (Sterwins 750 DW-3/1) pump. The set of components used to validate this approach and collect the data presented in this work are shown in Fig. 4.15. This setup is very robust and sufficient for the application [2].

Table 4.6 contains the basic parameters to all tests with the boost converter.

Table 4.6: Parameters attributed values.

Parameter	Description	Attributed value
P-01	Maximum Frequency	30 Hz
P-02	Minimum Frequency	50 Hz
P-03	Acceleration Ramp Time	5 s
P-04	Deceleration Ramp Time	5 s
P-07	Motor Rated Voltage	230 V
P-08	Motor Rated Current	5.4 A
P-09	Motor Rated Frequency	50 Hz
P-10	Motor Rated Frequency	2800 RPM
P-12	Primary Command Source	5 - PI Control
P-15	Digital Input Function Select	0
P-16	Analog Input 1 Signal Format	U 0-10 - Uni-polar 0-10 Volt Signal
P-30	Start Mode, Automatic Restart, ...	Auto-5
P-41	PI Controller Proportional Gain	30
P-42	PI Controller Integral Time	2
P-43	PI Controller Operating Mode	1 - Inverse Operation
P-44	PI Setpoint Source Select	1 - Analog Input 1 Setpoint
P-46	PI Feedback Source Select	3 - DC Bus Voltage

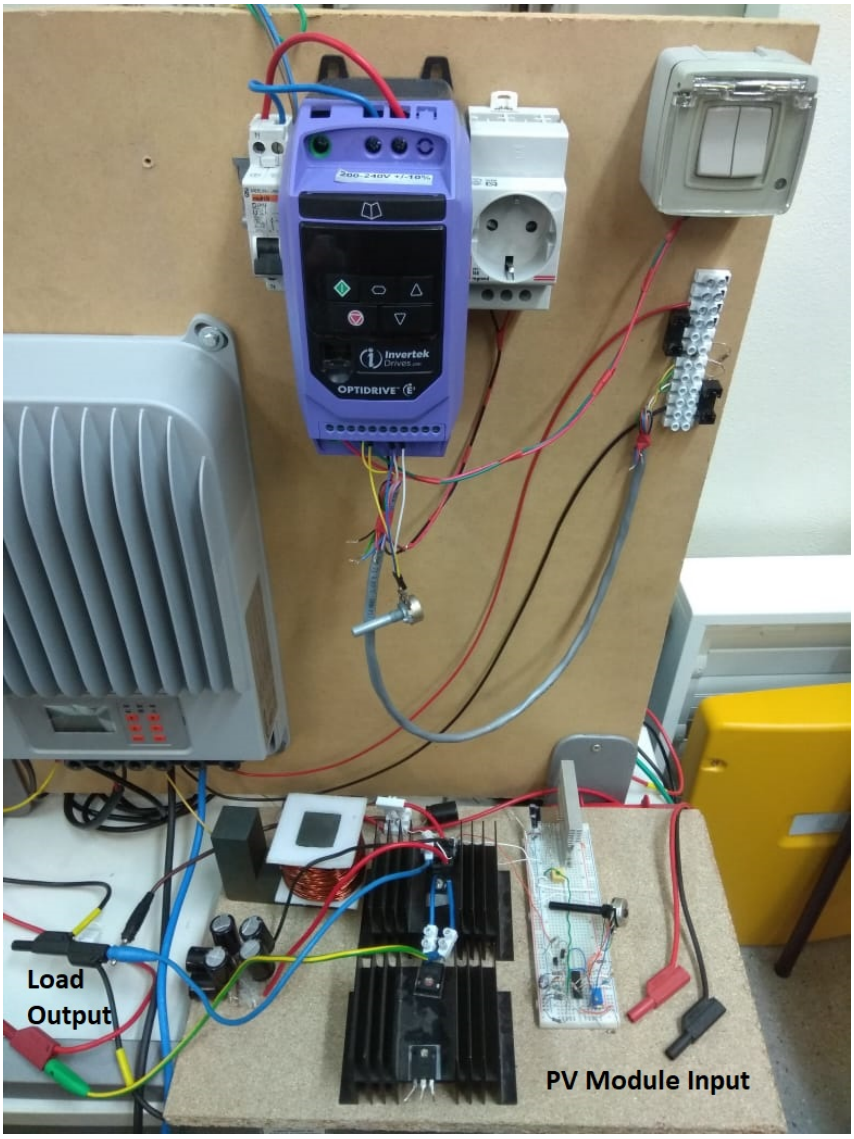

Figure 4.15: Experimental platform for low power applications based on the integration of a boost converter and a SFC.

The two goals of the PWM controller, as described in section 3 were achieved. Before the pump starts, the PWM controller TL494 limits the output voltage of the boost converter to the given maximum value (350 V) as shown in Fig. 4.16. During the normal operation of the pump, the output voltage of the boost converter is maintained constant by the SFC, as shown in Fig. 4.17. When the pump stops, for some reason, like an empty well or full tank, the TL494 does not let the output voltage of the boost converter be higher than the adjusted value, as can be seen in Fig. 4.18. The input voltage of the boost

converter is adjusted to be as close as possible to MPP voltage MPP when the pump is working, validating the control of the power in the boost converter. The voltage oscillation was seen in Fig. 4.16 and 4.18 can be mitigated by an improvement of the parametrization of the SFC [2].

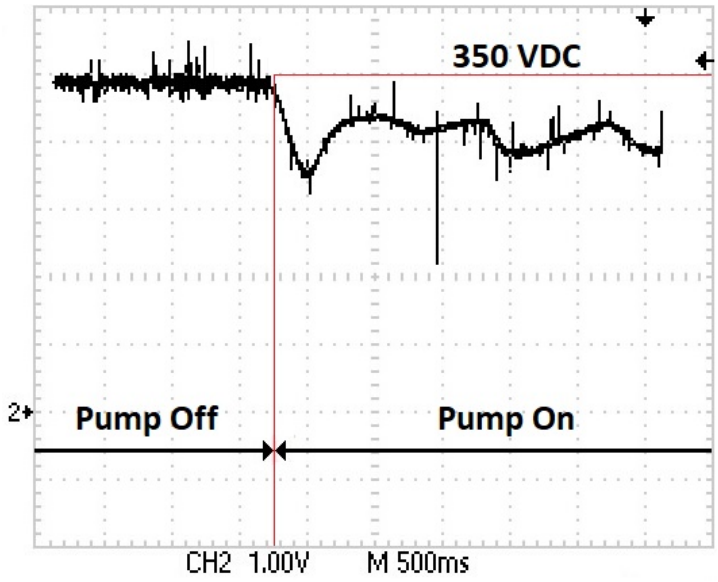

Figure 4.16: Voltage, seen throught a voltage divider, in the input of the SFC stable in 350 VDC before the pump starts

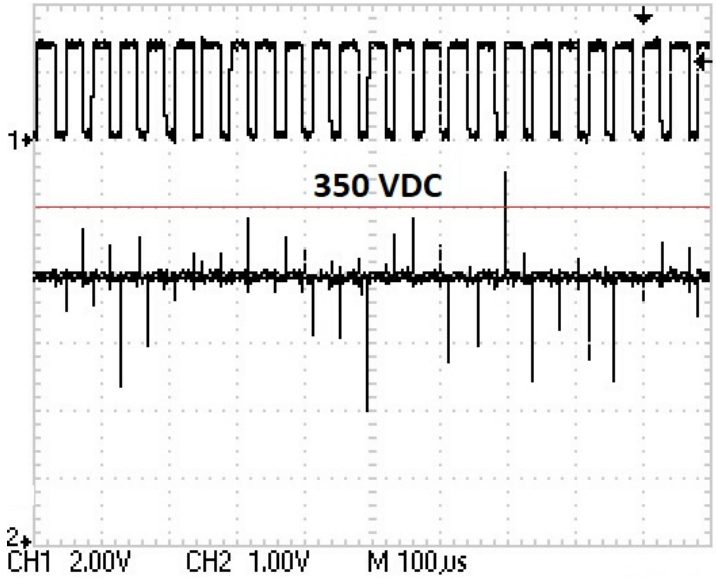

Figure 4.17: Voltage, seen throught a voltage divider, in the input of the SFC stable bellow 350 VDC with the pump working and the pulses in the IGBT

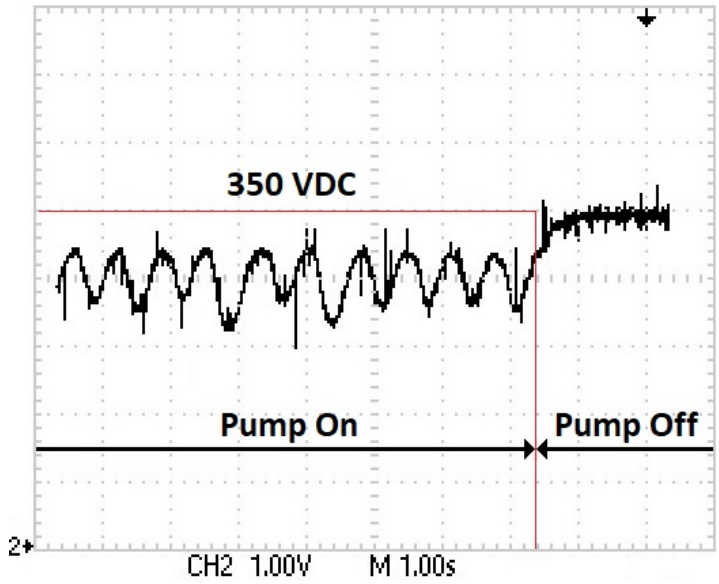

Figure 4.18: Voltage, seen throught a voltage divider, in the input of the SFC stable in 350 VDC after the pump stops

Fig. 4.19 represents one hour of operation. In this case, the pump worked from 15:00 to 16:00 as expected. It is possible to see that the control of the SFC is working according to the irradiation level. The values of the pump's frequency correspond to average values and the record of the radiation and frequency values are not exactly simultaneous [2].

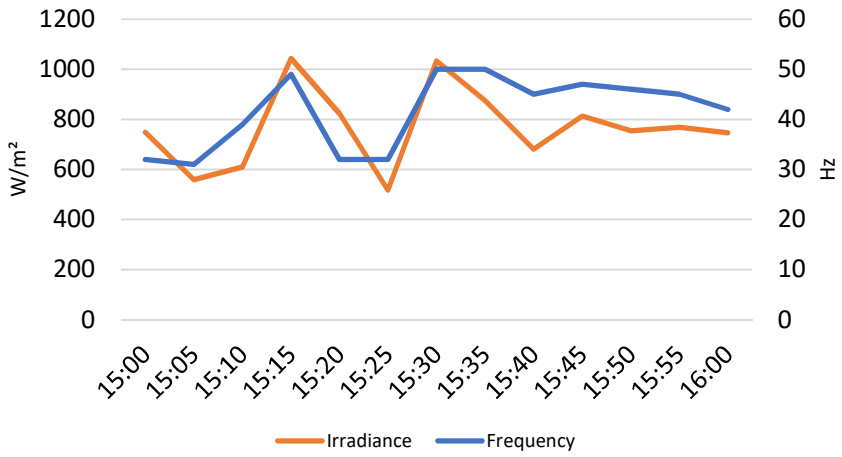

Figure 4.19: One hour of operation (irradiation and pump speed in Bragança at 15/05/2019) of a low power applications based on the integration of a boost converter and a SFC

Chapter 5

Conclusions and Future Work

The conclusions and future work, on the scope of development of new strategies for PVWPS based on standard components, are presented in this chapter.

5.1 Conclusions

This work described new reliable approaches for PVWPS based on SFC for low power levels (up to some hundreds of W). SFC and AC single-phase water pumps are reliable, off-the-shelf and cost-effective.

Indeed, a PV string can be directly connected to a SFC. However, a DC voltage of the order of magnitude of some hundreds of volts is needed even for low power levels. Therefore, several PV modules should be connected in series even for low power pumps, oversizing the PV string. This work proposed two new approaches for low power applications up to several hundreds of W. One is based on the integration of some (up to four) PV modules and standard components, namely, a charge controller with small capacity batteries, a battery inverter, a single-phase input/output SFC and a conventional single-phase AC pump. Additionally, a boost converter was developed and investigated as an alternative to the first one. This latter approach seems to be promising, according to the obtained results.

To validate the first approach were made seven tests, using a total of two models of

photovoltaic modules, two charge controllers, three battery models, five battery inverters, one single-phase input/output standard frequency converter and two AC pumps. Of these seven tests, four were completely successful, working proportionally to the irradiation using the battery voltage as setpoint or feedback, controlling the depth of discharge of the battery. The three that were not successful were due to the high inrush current of one of the pumps and the fact that some of the equipment available in the laboratory to the test was not ideal to the application.

To validate the second approach was used one model of a photovoltaic module, the boost converter designed and built in the work, one single-phase input/output standard frequency converter and one AC pump. This test was completely successful, working proportionally to the irradiation using the DC-link voltage as feedback.

These solutions are valuable for small and very small companies to develop their own cost-effective solutions due to the fact that one aproach uses only standard components that are widely available in the market and the other use a DC-DC converter that can be devoped in a integration between an education institution and a company. Actually, this work is being carried out in cooperation with the companies VALLED Soluções Energéticas and CHL Engenharia e Distribuição under regular cooperation activities.

5.2 Future Work

In the scope of this project, the potential future works are:

- Developement of other topologies of DC/DC converters.
- Analysis of the more suitable battery storage capacity, and characterization of energy storage in battery *versus* water in tank.
- Comparative price analysis between market solutions *versus* standard components.

Bibliography

[1] W. H. Organization, *Use of basic and safely managed drinking water services*, `http://www.who.int/gho/mdg/environmental_sustainability/water/en/`, 2018.

[2] A. K. Scortegagna, V. Leite, and D. Roman, "New approaches for low power photovoltaic water pumping systems", *Submited to IECON 2019 - 45th Annual Conference of the IEEE Industrial Electronics Society (IES)*, 2019.

[3] M. Alonso Abella, E. Lorenzo, and F. Chenlo, "Pv water pumping systems based on standard frequency converters", *Progress in Photovoltaics: Research and Applications*, vol. 11, no. 3, pp. 179–191, 2003.

[4] J. Fernández-Ramos, L. Narvarte-Fernández, and F. Poza-Saura, "Improvement of photovoltaic pumping systems based on standard frequency converters by means of programmable logic controllers", *solar energy*, vol. 84, no. 1, pp. 101–109, 2010.

[5] G. Li, Y. Jin, M. Akram, and X. Chen, "Research and current status of the solar photovoltaic water pumping system–a review", *Renewable and Sustainable Energy Reviews*, vol. 79, pp. 440–458, 2017.

[6] V. C. Sontake and V. R. Kalamkar, "Solar photovoltaic water pumping system-a comprehensive review", *Renewable and Sustainable Energy Reviews*, vol. 59, pp. 1038–1067, 2016.

[7] A. Barhdadi, "Photovoltaic water pumping systems in rural areas", *4th International Conference on Water Resources and Arid Environments (ICWRAE 4)*, pp. 836–843, Dec. 2010.

[8] T. S. P. D. Portal, *World, primary energy production*, http://www.tsp-data-portal.org/Energy-Production-Statistics#tspQvChart, Jun. 2019.

[9] A. Saadi and A. Moussi, "Neural network use in the mppt of photovoltaic pumping system", *Journal of Renewable Energy: ICPWE*, pp. 39–45, 2003.

[10] T. W. Bank, *Access to electricity, rural (% of rural population)*, https://data.worldbank.org/indicator/EG.ELC.ACCS.RU.ZS?most_recent_year_desc=true, Jun. 2019.

[11] T. Guardian, *Access to drinking water around the world – in five infographics*, https://www.theguardian.com/global-development-professionals-network/2017/mar/17/access-to-drinking-water-world-six-infographics, Jun. 2019.

[12] F. Carlevaro and C. Gonzalez, *Costing improved water supply systems for low-income communities: a practical manual*. IWA Publishing, 2015.

[13] P. E. Campana, "Pv water pumping systems for agricultural applications", PhD thesis, Mälardalen University, 2015.

[14] Y. H. Lim and D. Hamill, "Simple maximum power point tracker for photovoltaic arrays", *Electronics letters*, vol. 36, no. 11, pp. 997–999, 2000.

[15] D. J. V. Roman, "Photovoltaic Water Pumping Systems Based on Standard Components", Master's thesis, Instituto Politécnico de Bragança, Portugal, 2018.

[16] A. U. Brito and R. Zilles, "Systematized procedure for parameter characterization of a variable-speed drive used in photovoltaic pumping applications", *Progress in Photovoltaics: Research and Applications*, vol. 14, no. 3, pp. 249–260, 2006.

[17] Ultracell, *Ucg 12-20, specifications*, http://ultracell.co.uk/products/ucg-batteries/12v, Oct. 2018.

[18] Invertek, *Optidrive e3 user manual*, https://www.invertekdrives.com/client-uploads/download-manager/user-guides/GB_Optidrive_E3_User_Guide.pdf, Jun. 2019.

[19] jsdsolar, *Waterproof ip68 10a 15a 12v 24v wireless solar charge controller*, https://www.jsdsolar.com/solar-street-light-controller/Charge-Controller-12V-Street-Light.html, Jun. 2019.

[20] Epever, *Mppt it4415nd user manual*, https://www.epsolarpv.com/upload/file/1811/iTracer-AD-SMS-EL-V1.0.pdf, Jun. 2019.

[21] V. Leite, *Células e módulos fotovoltaicos*, Class Slides, Jun. 2019.

[22] I. Barbi and D. C. Martins, "Conversores cc-cc básicos não isolados", *Edição dos autores. CDU 621.314.22. Florianópolis.*, 2000.

[23] T. Instruments, *Tl494 pwm controller*, http://www.ti.com/lit/ds/symlink/tl494.pdf, Jun. 2019.

[24] Censi, *Torneira de boia para caixas d'água*, http://www.censi.com.br/produto/detalhe/torneira-de-boia-para-caixas-dgua-1, Jun. 2019.

Appendix A

Operation data from tests

Data from Sensor - Test F 02/04/19				Data From SFC		
TimeStamp	IntSolIrr	TmpAmb C	TmpMdul C	Time	Frequency	Pump Power
hh:mm	W/m^2	?C	?C	09:58:00	33	180
07:00	0,067	4,603	0,963	10:01:00	36,8	230
07:20	4,719	4,424	0,73	10:11:00	38,9	250
07:40	20,29	3,762	0,727	10:21:00	38	240
08:00	53,906	6,161	2,28	10:31:00	40,7	280
08:20	98,903	9,982	5,295	10:41:00	41	280
08:40	184,188	11,033	8,48	10:45:00	0	0
09:00	267,125	9,471	13,927	11:52:00	0	0
09:20	354,464	12,666	19,126	11:53:00	33	180
09:40	440,438	15,227	24,793	12:01:00	42,6	310
10:00	526,848	17,5	28,354	12:11:00	41	270
10:20	611,903	18,659	31,701	12:12:00	0	0
10:40	692,5	19,724	35,73	13:18:00	0	0
11:00	756,156	17,858	38,464	13:19:00	35	0
11:20	823,645	19,749	38,433	13:21:00	42,5	310
11:40	878,375	18,283	40,221	13:31:00	43,8	0
12:00	955,188	22,177	42,636	13:41:00	43,8	0
12:20	812,065	18,653	40,998	13:51:00	46,5	370
12:40	1000,13	18,258	41,793	14:01:00	46,5	370
13:00	1015,25	18,996	42,727	14:11:00	44	320
13:20	1012,65	18,511	39,672	14:21:00	45,2	340
13:40	1013,16	19,005	42,233	14:31:00	41,5	290
14:00	1014,88	19,033	37,414	14:41:00	46,2	360
14:20	994,484	18,772	36,398	14:51:00	45,8	350
14:40	978,594	18,527	34,202	15:01:00	44,6	330
15:00	938,75	18,599	34,021	15:11:00	44,9	330
15:20	904,516	18,214	32,027	15:21:00	44,7	330
15:40	856,75	18,427	32,193	15:31:00	42,8	300
16:00	792,781	18,221	29,864	15:41:00	43	310
16:20	706,032	18,743	31,069	15:51:00	43,1	310
16:40	626,844	18,258	28,549	16:01:00	42,5	300
17:00	497,781	18,005	26,093	16:11:00	41,8	290
17:20	421,194	17,378	23,195	16:21:00	40,3	270
17:40	349,667	17,239	21,885	16:31:00	37,5	230
18:00	230,156	16,577	20,064	16:41:00	38,9	250
18:20	185,839	16,272	18,63	16:51:00	37,6	230
18:40	130,172	16,154	17,533	17:01:00	34,6	200
19:00	68,152	15,709	15,73	17:11:00	32,8	180
19:20	32,75	15,864	14,214	17:21:00	31,4	170
19:40	10,406	14,546	13,114	17:30:00	30	160
20:00	0,031	13,643	11,736	17:31:00	0	0

Data from Sensor - Test F 02/05/19				Data from SFC		
Time	IntSolIrr	TmpAmb C	TmpMdul C	Time	Freq	Pump Power
hh:mm	W/m^2	?C	?C	09:33	37	240
07:00	26,355	7,301	3,459	09:43	38,6	250
07:20	39,281	10,705	4,877	09:53	39,1	260
07:40	68,844	11,133	7,008	10:03	40,3	280
08:00	127,938	11,005	9,564	10:13	41	290
08:20	205,531	11,236	11,796	10:23	41,3	290
08:40	293,281	12,852	14,839	10:33	41,4	290
09:00	372,406	11,933	16,749	10:43	42,3	310
09:20	487,219	13,664	19,464	10:53	42	310
09:40	594,406	13,721	23,477	11:03	42,3	310
10:00	645,226	15,478	26,649	11:13	42,5	310
10:20	739,484	14,42	28,375	11:23	41,7	300
10:40	809,719	14,452	29,446	11:33	42,1	300
11:00	822,516	15,088	31,875	11:43	42	300
11:20	869,129	16,707	34,091	11:53	42,5	310
11:40	920,281	19,168	35,899	12:03	42,5	310
12:00	989,469	17,899	37,699	12:13	41,5	300
12:20	1023,125	17,264	39,674	12:23	42,8	320
12:40	1049,844	17,061	40,643	12:33	42	300
13:00	1052,129	20,23	45,898	12:43	41,9	300
13:20	1064,656	18,874	45,086	12:53	41,5	300
13:40	1025,29	21,24	47,862	13:03	42,1	290
14:00	1030,839	19,136	44,569	13:13	41,3	290
14:20	993,75	20,983	45,024	13:23	40,9	290
14:40	963,656	21,546	49,464	13:33	41	290
15:00	969,063	21,252	45,624	13:43	41,2	290
15:20	752,406	21,274	44,871	13:53	41	290
15:40	597,844	20,521	37,73	14:03	41,1	290
16:00	666,839	23,014	42,94	14:13	40	270
16:20	631,065	21,653	34,062	14:23	40	270
16:40	669,667	21,669	40,188	14:33	40,7	280
17:00	579,71	22,404	37,782	14:43	40,9	280
17:20	464,563	20,511	34,064	14:53	40,5	280
17:40	356,313	21,943	31,686	15:03	40	270
18:00	240,406	21,821	27,574	15:13	39,2	260
18:20	136,125	21,124	23,952	15:23	39,4	260
18:40	213,226	24,646	24,759	15:33	39,3	260
19:00	97,645	23,627	23,682	15:43	39,5	260
19:20	76	22,983	20,83	15:53	39	260
19:40	66,613	22,714	20,204	16:03	38,8	260
20:00	23,677	19,314	18,211	16:13	38,3	250
				16:23	37,7	240

Data from Sensor - Test G 13/05/19				Data from SFC	
Time	IntSolIrr	TmpAmb C	TmpMdul C	Time	Freq
hh:mm	W/m^2	?C	?C	09:32	36
09:30	525,938	20,133	27,418	09:42	36,9
09:35	547,71	19,649	27,982	09:52	38,2
09:40	569,063	20,536	28,899	10:02	38,9
09:45	590	20,464	29,414	10:12	39,8
09:50	610,355	20,311	29,649	10:22	40,6
09:55	630,576	20,563	30,509	10:32	41
10:00	649,938	19,964	31,864	10:42	41,6
10:05	669	19,865	32,288	10:52	41,9
10:10	687,188	21,399	33,621	11:02	42,3
10:15	703,969	20,746	34,711	11:12	42,6
10:20	720,719	21,346	35,749	11:22	42,7
10:25	739,344	21,33	35,733	11:32	43
10:30	757,156	21,108	35,98		
10:35	776,516	20,327	34,817		
10:40	795,219	21,024	34,946		
10:45	808,281	22,452	37,099		
10:50	822,839	21,53	37,517		
10:55	839,938	21,902	36,824		
11:00	851,906	23,043	38,749		
11:05	864,483	23,313	39,213		
11:10	880,424	22,951	38,763		
11:15	893,281	24,049	39,593		
11:20	905,194	23,185	39,911		
11:25	916,031	24,549	41,411		
11:30	925,938	23,633	41,964		
11:35	937,258	24,778	41,707		

Data from Sensor - Test Boost - 15/05/19				Data from SFC	
TimeStamp	IntSolIrr	TmpAmb C	TmpMdul C	Time	Freq
hh:mm	W/m^2	?C	?C	15:00	32
15:00	749,097	31,075	48,746	15:05	31
15:05	559,469	30,852	45,893	15:10	39
15:10	609,839	31,043	42,656	15:15	49
15:15	1043,344	31,424	46,886	15:20	32
15:20	824,323	31,365	49,911	15:25	32
15:25	517,625	30,658	44,243	15:30	50
15:30	1033,548	31,165	46,401	15:35	50
15:35	875,219	31,78	50,277	15:40	45
15:40	681,323	30,478	47,117	15:45	47
15:45	813,281	30,358	44,633	15:50	46
15:50	754,625	30,577	45,38	15:55	45
15:55	768,774	30,282	44,385	16:00	42
16:00	746,563	30,199	44,433		